QCD in finite volume

Sasa Prelovsek

University of Ljubljana

Jozef Stefan Institute, Ljubljana, Slovenia

University of Regensburg

EuroPLEx School, fall 2020

Motivation

outline will be presented after motivation

Clasification of hadron states

these lectures: QCD, no electro-weak interactions, only strong decays

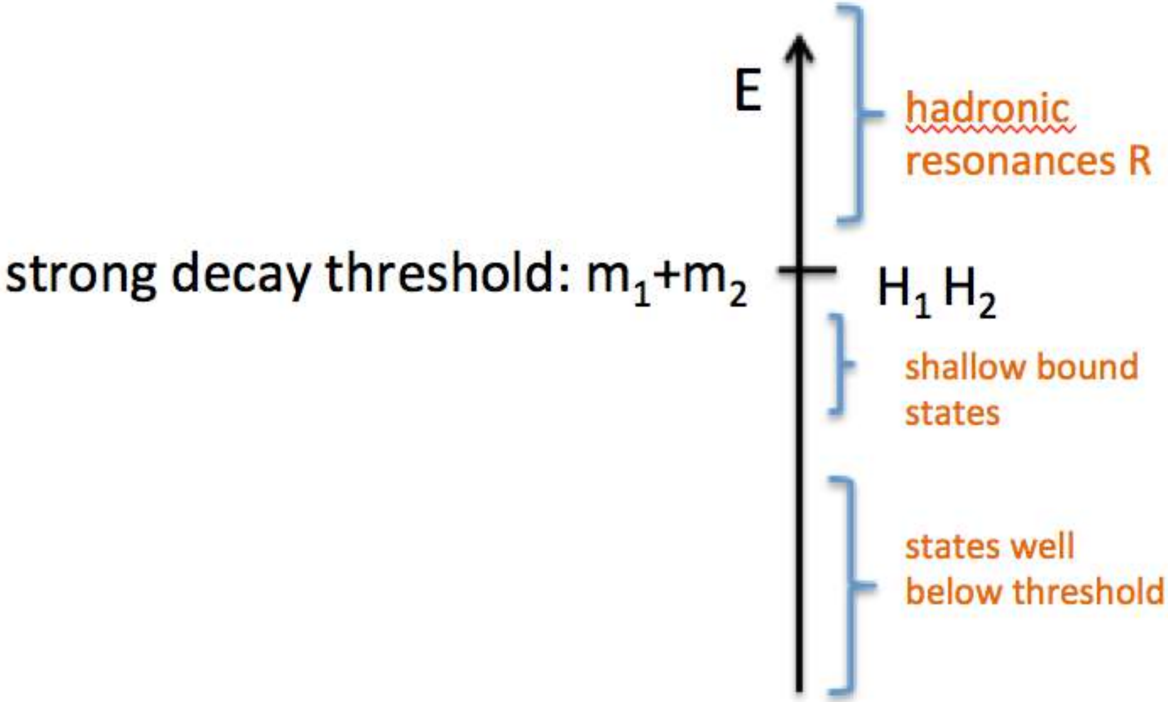

decay strongly

not eigenstates of QCD

can not decay strongly:

p n D D* D K

deuteron, X(3872), D_{s0}*(2317)

Mesonic resonance and bound states

- states well below threshold
- strongly decay: resonances
- candidates for shallow bound st.

(analogues of deuterium)

$\bar{u}u$

$\pi^\pm$
π^0
η
$f_0(500)$ or σ was $f_0(60$
$\rho(770)$
$\omega(782)$
$\eta'(958)$
$f_0(980)$
$a_0(980)$
$\phi(1020)$
$h_1(1170)$
$b_1(1235)$
$a_1(1260)$
$f_2(1270)$
$f_1(1285)$
$\eta(1295)$
$\pi(1300)$
$a_2(1320)$
$f_0(1370)$
$h_1(1380)$
$\pi_1(1400)$
$\eta(1405)$
$f_1(1420)$
$\omega(1420)$
$f_2(1430)$
$a_0(1450)$
$\rho(1450)$

$\bar{s}u$

$K^\pm$
K^0
$K_S{}^0$
$K_L{}^0$
$K_0^*(800)$ or κ
$K^*(892)$
$K_1(1270)$
$K_1(1400)$
$K^*(1410)$
$K_0^*(1430)$
$K_2^*(1430)$
$K(1460)$
$K_2(1580)$
$K(1630)$
$K_1(1650)$
$K^*(1680)$
$K_2(1770)$
$K_3^*(1780)$
$K_2(1820)$
$K(1830)$

$\bar{c}u$

$D^\pm$
D^0
$D^*(2007)^0$
$D^*(2010)^\pm$
$D_0^*(2400)^0$
$D_0^*(2400)^\pm$
$D_1(2420)^0$
$D_1(2420)^\pm$
$D_1(2430)^0$
$D_2^*(2460)^0$
$D_2^*(2460)^\pm$
$D(2550)^0$
$D(2600)$
$D^*(2640)^\pm$
$D(2750)$

$\bar{c}s$

$D_s^\pm$
$D_s^{*\pm}$
$D_{s0}^*(2317)^\pm$ slightly below DK
$D_{s1}(2460)^\pm$ D*K
$D_{s1}(2536)^\pm$
$D_{s2}^*(2573)$
$D_{s1}^*(2700)^\pm$
$D_{s1}^*(2860)^\pm$
$D_{s3}^*(2860)^\pm$
$D_{sJ}(3040)^\pm$

Hadronic resonances appear in scattering as "bumps" in cross-section

decay time (via strong int.) : τ

uncertainty in E: $\Gamma = \hbar / \tau$

Γ=1–300 MeV

Example: ρ

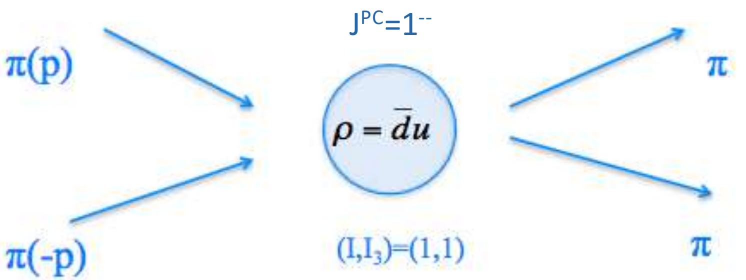

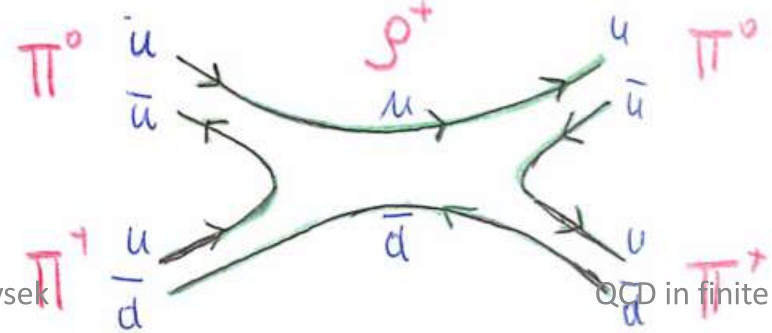

in experiment and in theory one determines:

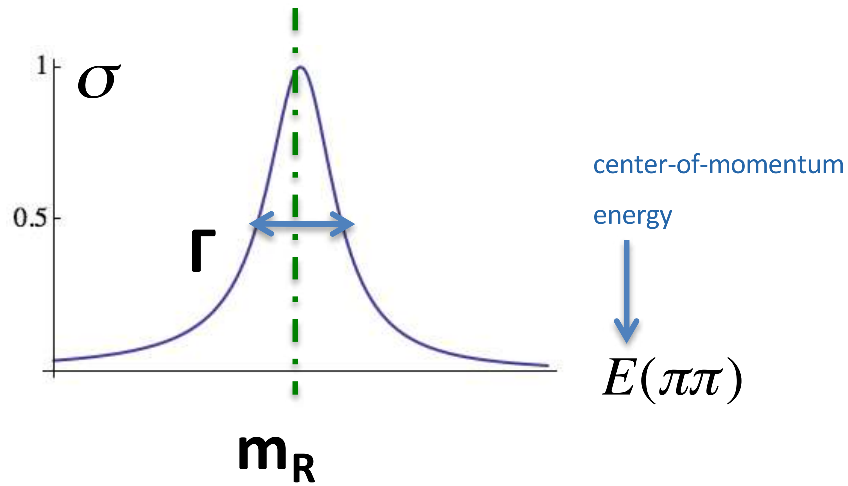

$$\sigma(E) \propto |T(E)|^2 = \left|\frac{E\Gamma}{E^2 - m_R^2 + iE\Gamma}\right|^2$$

simplest Breit Wigner

scattering amplitude

Some examples from experiment

https://lhcb-public.web.cern.ch

there is great data from other exps as well!

Cconventional charmonium resonances: c c

LHCb 2019
1903.12240

J^{PC} 1^{--} 3^{--} 2^{++}

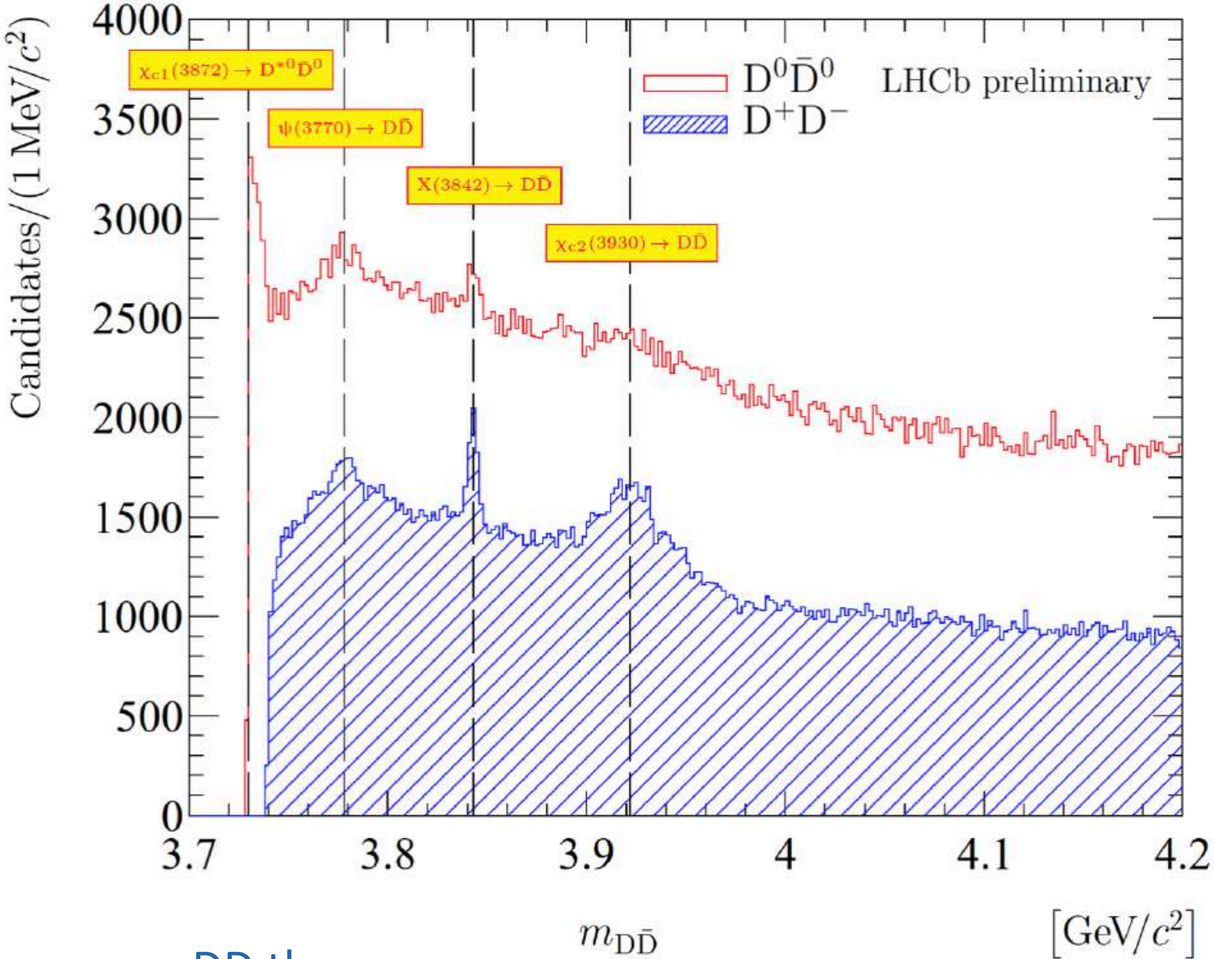

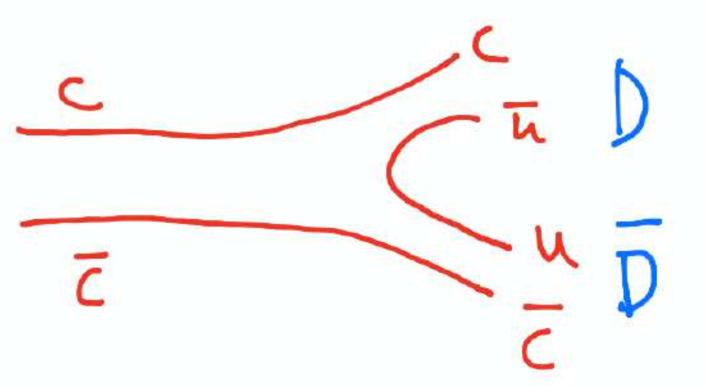

DD th.

Candidates for conventional hadrons: excited Ω_c^*

LHCb march 2017
1703.04639

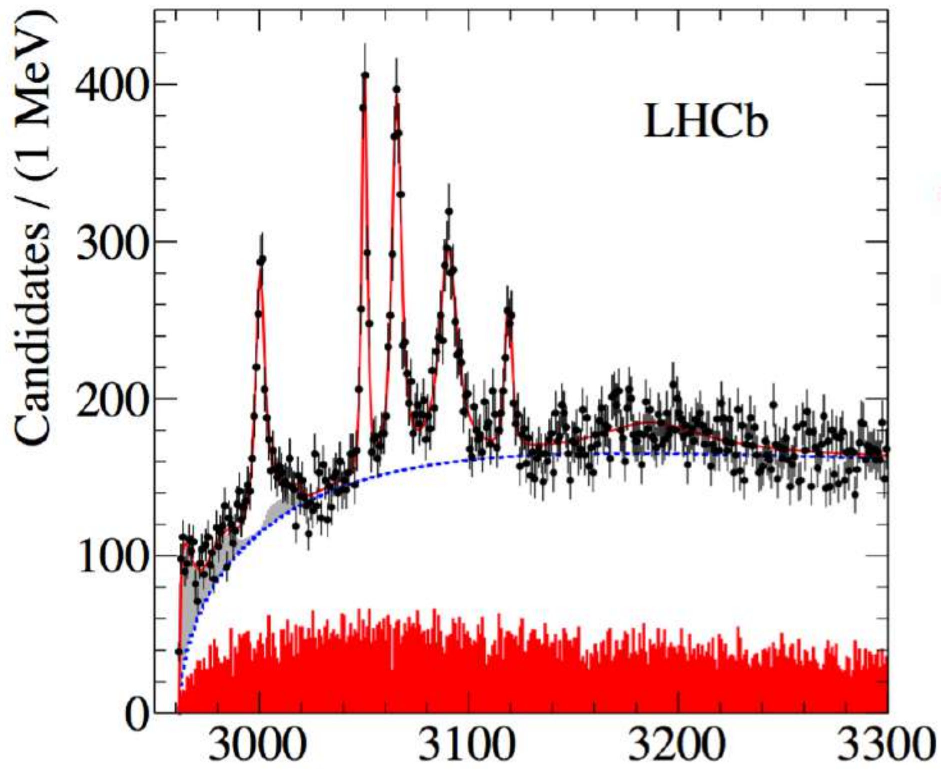

$$E(\Xi_c^+\ K^-)\ [GeV]$$

$$\Omega_c^* \to \Xi_c^+\ K^-$$

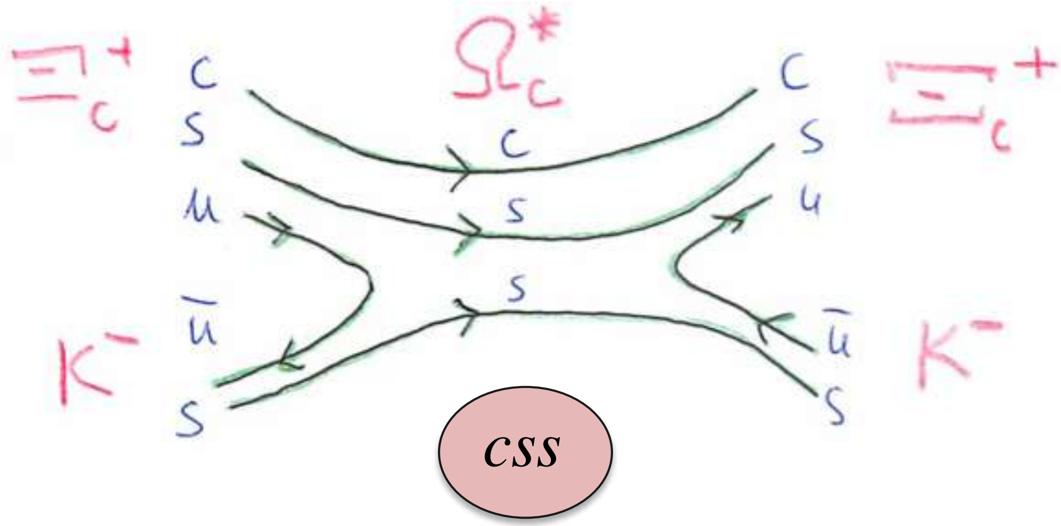

five narrow resonances

Candidates for exotic hadrons: pentaquarks P_c

LHCb 2019

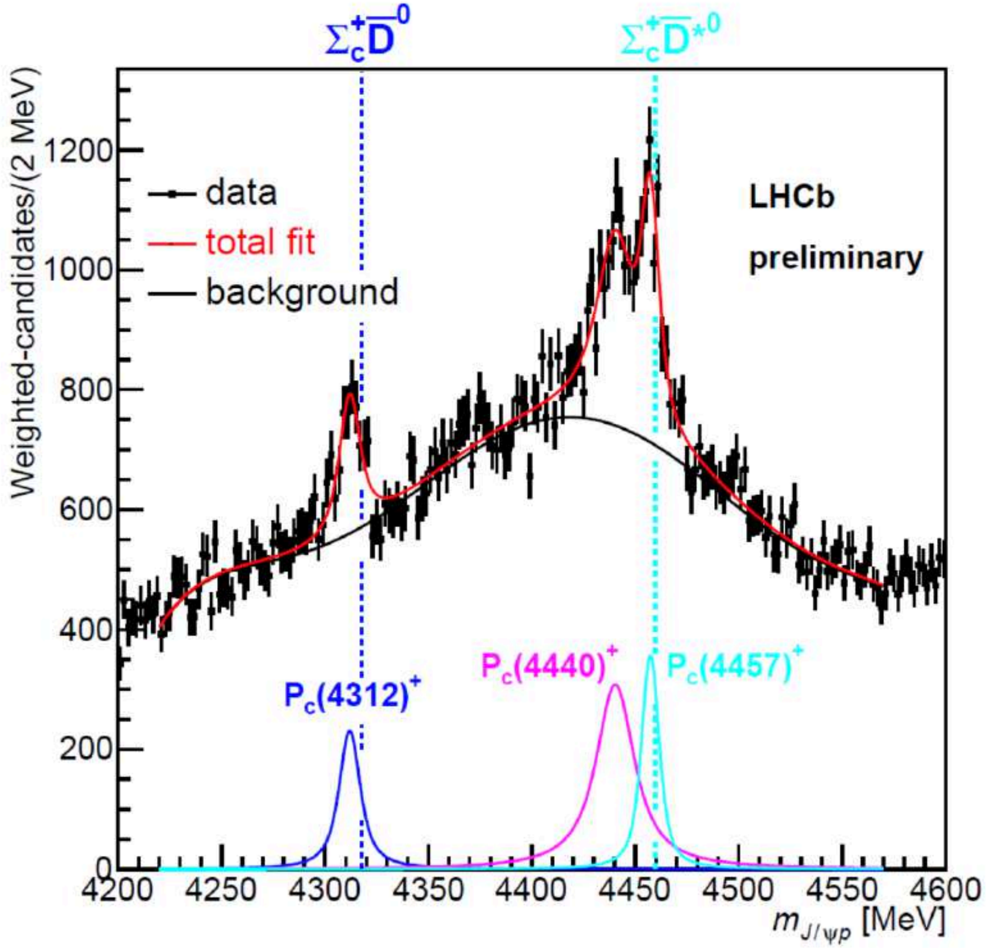

$$E(J/\psi\ p)\ [GeV]$$

$$P_c^+ \to J/\psi \ \ p$$

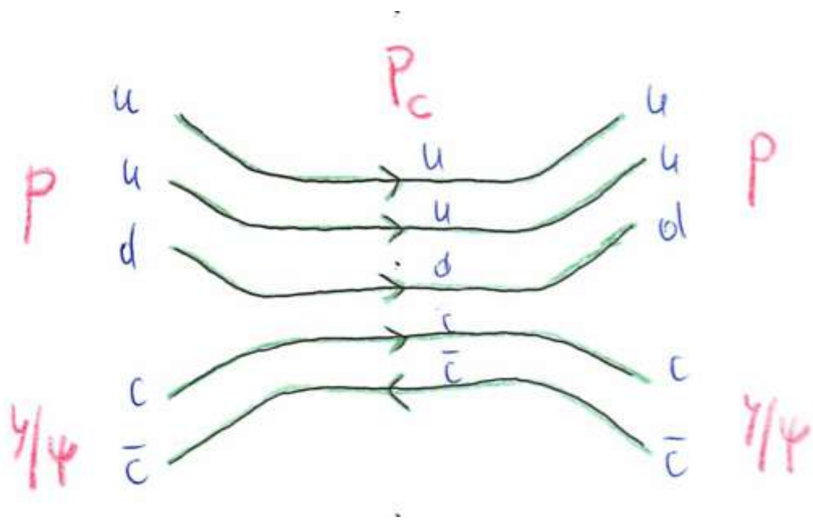

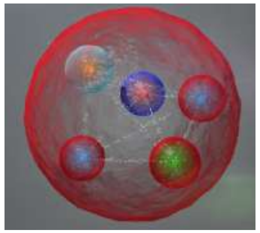

Fully charming tetraquark: $\underline{c}$ c $\underline{c}$ c

LHCb 2020

2006.16957

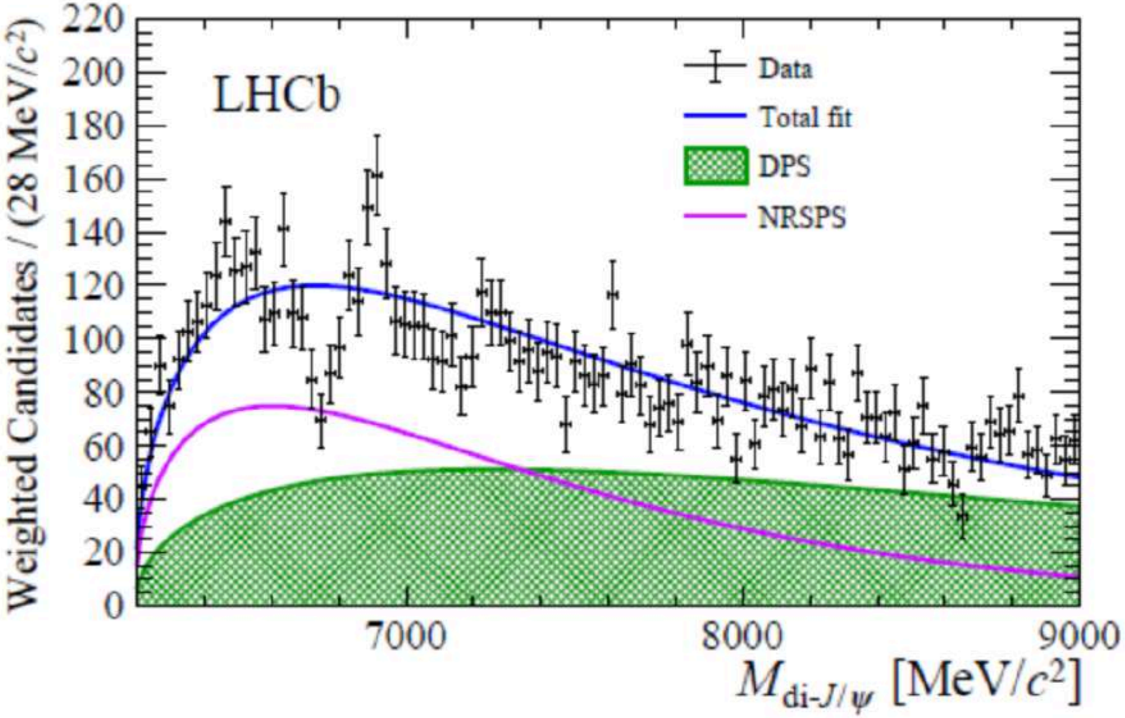

X(6900)

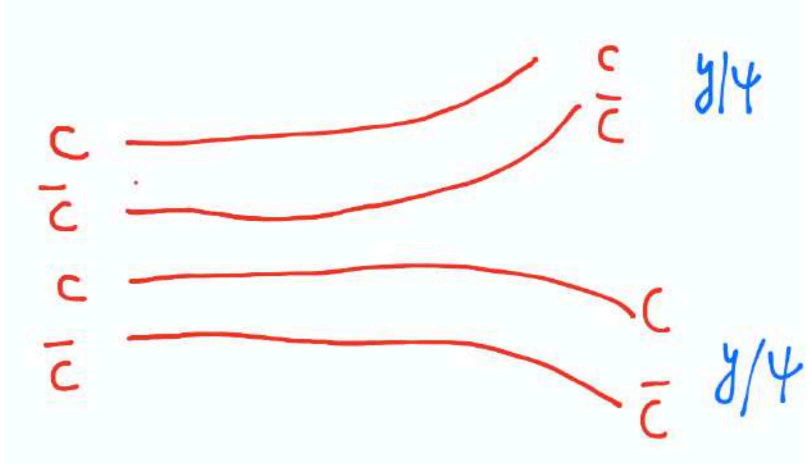

Candidates for exotic hadrons: tetraquarks Z_c^+

[BESIII & Belle 2013, PRL]

Example: $Z_c^+(3900)$

$$Z_c^+(3900) \rightarrow J/\psi\ \pi^+$$

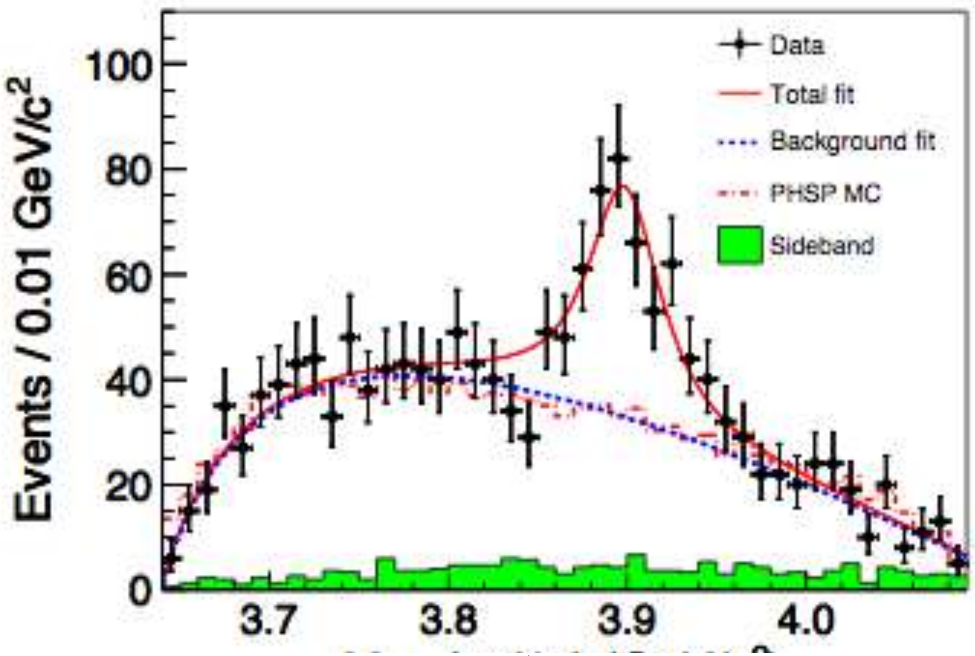

$$E(J/\psi\ \pi^+)\ [GeV]$$

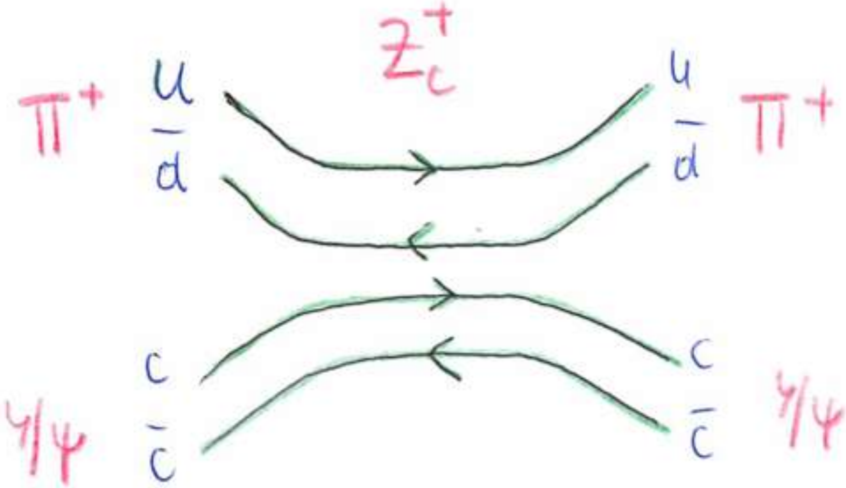

$$\begin{matrix} \bar{c} & u \\ c & \bar{d} \end{matrix}$$

M ≈ 3900 MeV , Γ ≈ 30 MeV

a number of other exotic hadrons were discovered in past fourteen years ..

Outline for all lectures

1. scattering in continuum

- shallow bound states, virtual bound states, resonances
- poles of scattering amplitude T in complex energy-plane ...

2. lattice QCD in finite volume

- extracting eigen-energies E_n of two-hadron system
- derivation of Luscher's relation between E_n and scattering matrix T in QFT

3. (simple) examples: lattice studies of one-channel scattering

- bound states, virtual bound states, resonances

4. scattering of particles with spin: construction of two-hadron interpolators

coupled-channel scattering

Disclaimer

The lectures do not present review of lattice simulations

Specific lattice results are shown just as examples

Often results based on less fancy analysis are presented for simplicity

For an overview of the literature: consult papers or review papers

Scattering processes and resonances from lattice QCD
R. Briceno, J. Dudek, R. Young
1706.06223, Rev. Mod. Phys

The *XYZ* states: experimental and theoretical status and perspectives
N. Brambilla, S. Eidelman, C. Hanhart, A. Nefediev, C.-P. Shen, C. Thomas, A. Vairo, C.-Z. Yuang
1907.07583, Physics Reports
(there is section on lattice results)

The Belle II Physics book, Quarkonium(like) Physics (chapter 14)
N. Brambilla, B. Fulsom, C. Hanhart, Y. Kiyo, R. Mizuk, R. Mussa, A. Polosa, S. Prelovsek, C. P. Shen
1808.10567, Progress of Theoretical and Experimental Physics
(there is section on lattice results)

Lattice sectroscopy with focus on exotics
S. Prelovsek
2001.01767, PoS Beauty 2019

proceedings of Lattice conferences, paralell or plenary talks

.....

Outline, lecture 1

T=scattering amplitude

Scattering in continuum

- shallow bound states, virtual bound states, resonances
- how do we identify them once T is extracted
- poles of T in complex energy-plane, Riemann sheets
- partial waves : l=0, l>0
- near-threshold behavior
- example: spherical well potential

Hadrons

Conventional

valence quark

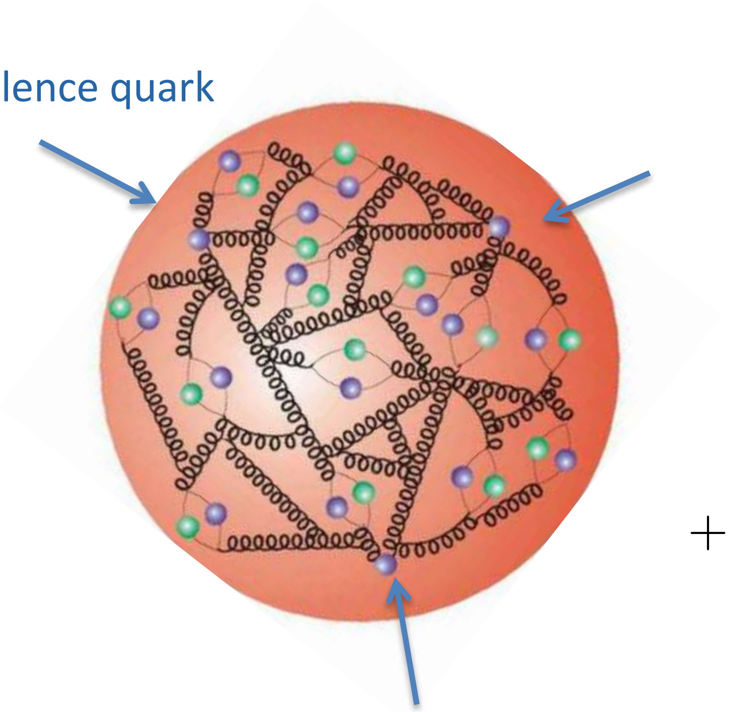

$+$ glons

$+ \bar{q}q$ pairs

Exotic

minimal valence content

$\bar{q}\ \bar{q}\ q\ q$ tetraquarks

$\bar{q}\ q\ q\ q\ q$ pentaquarks

$\bar{q}\ q\ G$ hybrid mesons

all exp discovered exotic hadrons

are resonances or shallow bound states

Terminology in this talk: tetra(penta) quarks indicate just the number of valence quarks in the state; it is not meant to say anything on how quarks are clustered in them

Current status

exp. discovered exotic hadrons

P_c , Z_c , X(6900), ...

$\longleftrightarrow$

not easy for lattice QCD

(several strong decay channels)

some exotic hadrons identified on lattice

b b $\underline{u}$ $\underline{d}$, b b $\underline{u}$ $\underline{s}$

$\longleftrightarrow$

(too) difficult for experiment

those two not discovered yet

many challenges left

experimental progress and results are impressive and motivating

Scattering in Nonrelativistic Quantum Mechanics

Schrodinger equation

$$\left[-\frac{\hbar^2}{2m}\left(\frac{\partial^2}{\partial r^2}+\frac{2}{r}\frac{\partial}{\partial r}\right)+\frac{\boldsymbol{L}^2}{2mr^2}+V(r)\right]\psi(r,\vartheta,\varphi)=E\psi(r,\vartheta,\varphi)\,.$$

$$\psi(r,\vartheta,\varphi)=R(r)\,Y_{lm}(\vartheta,\varphi) \qquad R(r)=u(r)/r$$

$$\left[-\frac{\hbar^2}{2m}\frac{d^2}{dr^2}+\frac{\hbar^2 l(l+1)}{2mr^2}+V(r)\right]u(r)=Eu(r)$$

R=relative distance

m=reduced mass

Scattering

Schwabl, Chapter 18

$$\psi(x) = e^{i\vec{p}\cdot\vec{x}} + \frac{f(\theta)}{r} e^{ipr}$$

for large r

In (e^{-ipr})+ out (e^{ipr}) Only out

$$\frac{d\sigma}{d\Omega} = \frac{dN}{N_{in}\ d\Omega} = |f(\theta)|^2$$

Plot of V(r)

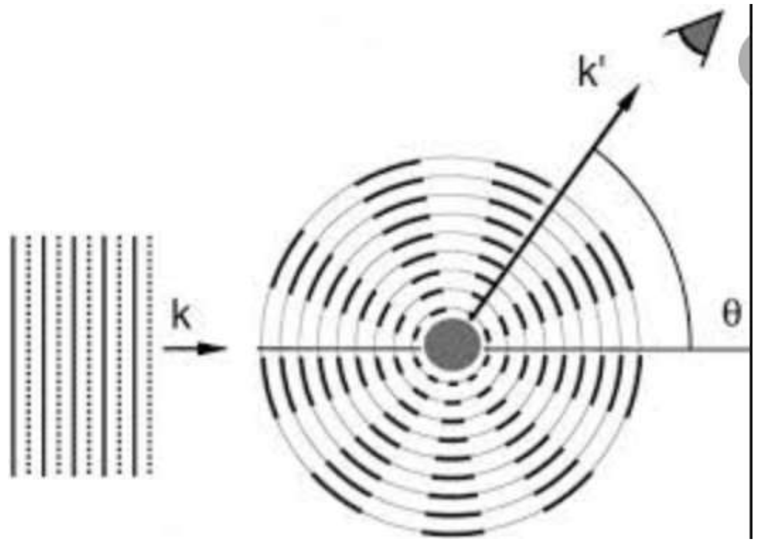

Scattering, l=0 (s-wave)

Schwabl, chapter 18.3

dominant at small E

$$\psi(x) \propto e^{i\vec{p}\cdot\vec{x}} + \frac{f(\theta)}{r} e^{ipr}$$

in (e^{-ipr}) only in the first term

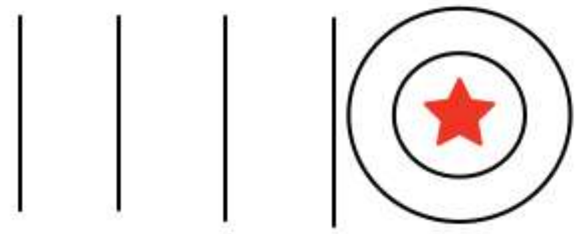

if λ >> object (low p) : s-wave dominant

on the other hand, for r>R where V(r)=0:

$$\left[-\frac{\hbar^2}{2m}\frac{d^2}{dr^2} + \underbrace{\frac{\hbar^2 l(l+1)}{2mr^2} + V(r)}_{0} \right] u(r) = Eu(r)$$

$$u(r) = A\ \sin(pr + \delta_0)$$

$$u(r) \propto \sin(pr+\delta_0) = \frac{1}{2i}[e^{ipr+i\delta_0} + e^{-ipr-i\delta_0}]$$

$$= \frac{e^{-i\delta_0}}{2i}[\underbrace{e^{+2i\delta_0}}_{S(E)}\ e^{ipr} + e^{-ipr}]$$

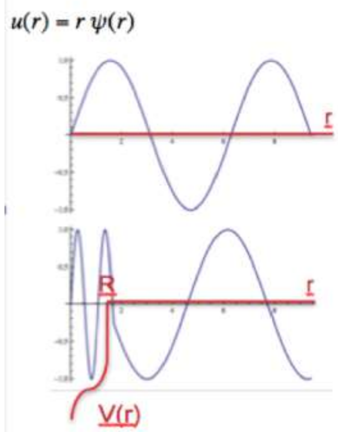

QM interpretation:

$$\psi(r) \propto \frac{\sin(pr)}{r}$$

$$\psi(r) \propto \frac{\sin(pr+\delta)}{r} \qquad r > R$$

unknown $\qquad r < R$

complicated

S=<out|in>

$$S(E) = e^{2i\delta_0(E)}\ , \qquad S^\dagger S = I$$

conservation of prob.

Scattering, l=0 (s-wave)

Schwabl, chapter 18.3

dominant at small E

$$\psi(x) \propto e^{i\vec{p}\cdot\vec{x}} + \frac{f(\theta)}{r} e^{ipr}$$

in (e^{-ipr}) only in the first term

on the other hand, for r>R where V(r)=0:

$$\left[-\frac{\hbar^2}{2m}\frac{d^2}{dr^2} + \underbrace{\frac{\hbar^2 l(l+1)}{2mr^2}}_{0} + V(r) \right] u(r) = E u(r)$$

$$u(r) = A \; \sin(pr + \delta_0)$$

$$f_{l=0} = \frac{e^{2i\delta_0} - 1}{2i \; p}$$

plot of s-wave scat

Scattering, l=0 (s-wave)

$$f_{l=0} = \frac{e^{2i\delta_0} - 1}{2i\, p}$$

different normalizations of T are used

$$S(E) = e^{2i\delta_0(E)} = I + 2ip\, f(E) = I + 2ip\, T(E)\ , \quad f(E) = T(E)$$

$$T = \frac{e^{2i\delta_0} - 1}{2i}\, \frac{1}{p} = e^{i\delta_0} \sin \delta_0\, \frac{1}{p} = \frac{1}{\cot \delta_0 - i}\, \frac{1}{p}$$

$$\boxed{T = \frac{1}{p \cot \delta_0 - ip}}$$

T= scattering amplitude:

basic object of these lectures

$$\sigma = 4\pi\, |f|^2 = 4\pi \frac{\sin^2 \delta_0}{p^2}$$

Spherical well in 3D : bound state (l=0)

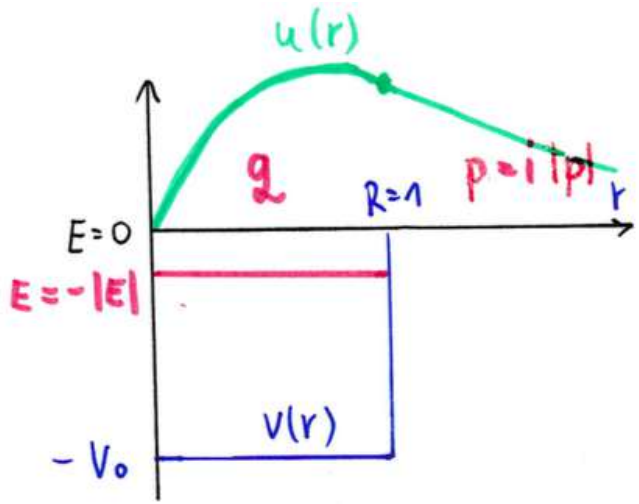

$$A\ \sin qr \qquad B\ e^{-|p|r}$$

$$\psi(r) = R(r) = \frac{u(r)}{r} \qquad (l=0)$$

$$\left.\begin{aligned} u(R) &= A\ \sin qR = B\ e^{-|p|R} \\ u'(R) &= qA\cos qR = -\,|\,p\,|\,B\ e^{-|p|R} \end{aligned}\right\} \quad \frac{1}{q}\tan qR = -\frac{1}{|\,p\,|} \longrightarrow$$

example: deuterium (pn, J=1)

V0=36 MeV, R=2 fm, $m=m_N/2$

$E = E_B = -2\ MeV$

$q^2/2m = E + V0$ $\qquad p^2/2m = E < 0$

$p=+\,i\,|p|$: we will call this Riemann sheet 1, Im(p) > 0

Aim: show that scattering matrix $T(E=E_B) = \infty$ at the energy of the bound state on Riemann sheet 1

spherical well: scattering with l=0

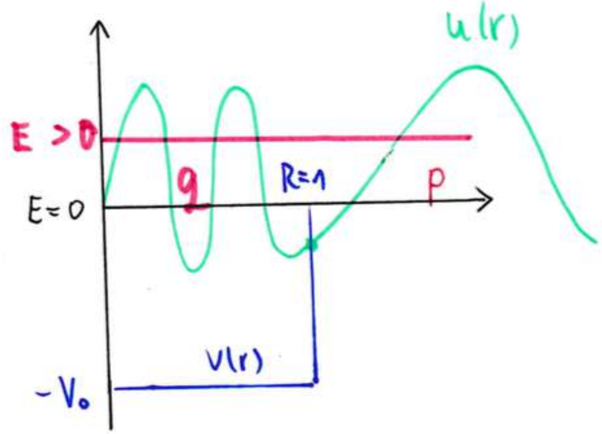

$$A \sin qr \qquad B \sin(pr + \delta_0)$$

E > 0 : scattering

relations apply also for E < 0

p: momontum of a scattering particle in cmf

$$\left.\begin{array}{l} u(R) = A \sin qR = B \sin(pR + \delta) \\ u'(R) = q\, A \cos qR = p\, B \cos(pR + \delta) \end{array}\right\}$$

dividing both eqs $\quad \frac{1}{q} \tan qR = \frac{1}{p} \tan(pR + \delta)$

$$\boxed{\delta_0(p) = \arctan\left(\frac{p}{q}\tan(qR)\right) - pR + n\pi}$$

example: deuterium (pn, J=1)

V0=36 MeV, R=2 fm, $m_r = m_N/2$

E = $E_B = -2\ MeV$

$$\boxed{T = \frac{1}{p \cot \delta_0 - ip}}$$

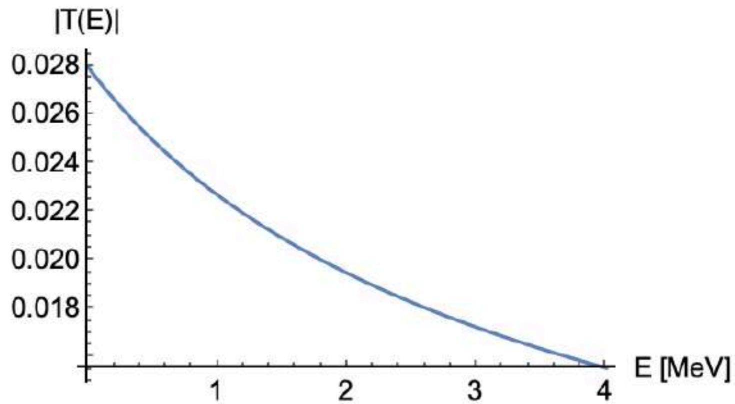

Bound state

bound state corresponds to a pole of the scattering matrix $T(E=E_B) = \infty$ below threshold

for p= i |p| (Riemann sheet 1)

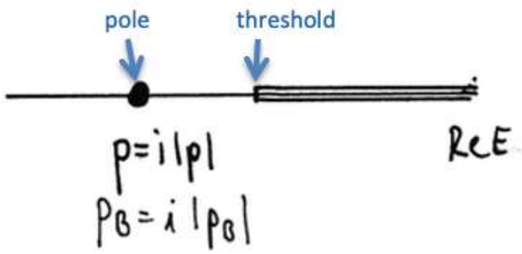

example: deuteron (pn, J=1)

V0=36 MeV, R=2 fm, $m_r=m_N/2$

$E = E_B = -2\ MeV$

$E=p^2/2m$, $p=\pm\, i\sqrt{2m|E|}$, take +

$$\boxed{T = \frac{1}{p\cot\delta_0 - ip}}$$

the plot below indicates a pole for p=i |p| (sheet 1)

pole of T at the position of the bound state

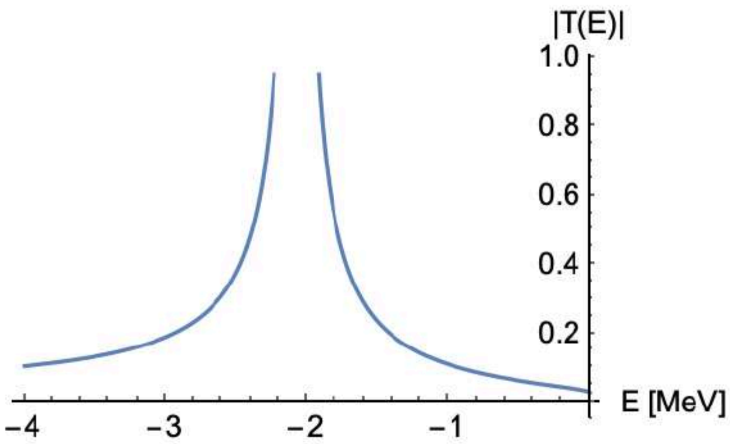

extracted from lat

p cot(del) [blue] ; i p = – |p| [orange]

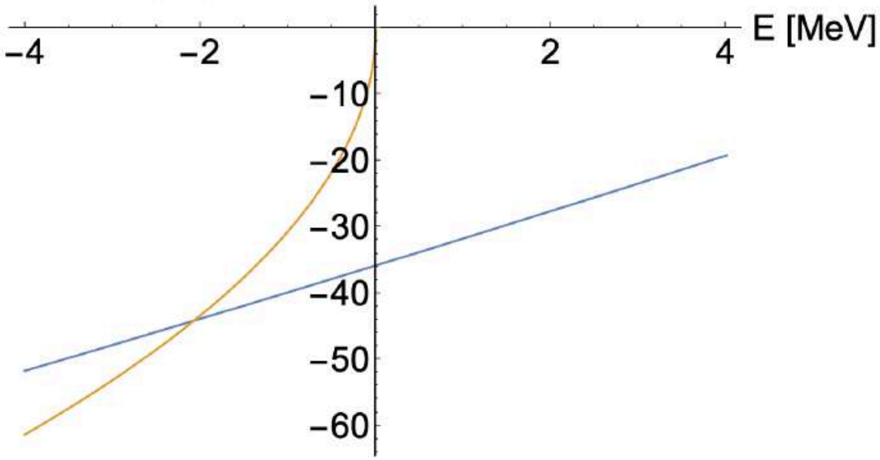

Bound state in QM

$$u(r) \propto \sin(pr + \delta_0) \propto e^{ipr+i\delta_0} + e^{-ipr-i\delta_0} \propto e^{+2i\delta_0}\, e^{ipr} + e^{-ipr}$$

r>R

S= ∞, $p = i\,|p|$

only exp falling part

Bound state in QFT

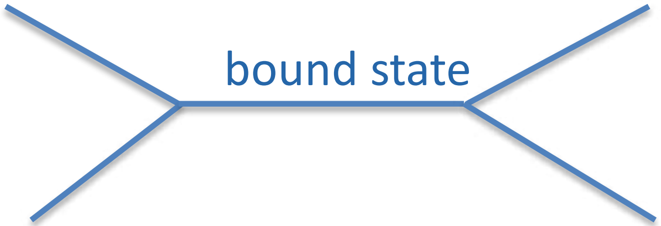

$$\mathrm{T(E)} \propto \frac{1}{s-m^2} = \frac{1}{E_{cm}^2-m^2}$$

$\mathrm{T}(E_{cm} = m) = \infty$

scattering matrix has a pole $T(E=E_B) = \infty$

at the energy of the bound state

Virtual bound state

bound state corresponds to a pole of the scattering matrix $T(E=E_B) = \infty$ below threshold for $p= -i\ |p|$ (Riemann sheet 2)

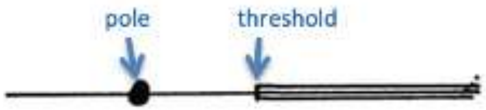

$p= -i\ |p|$

more on Riemann sheets- in few slides

$$T = \frac{1}{p\cot\delta_0 - ip}$$

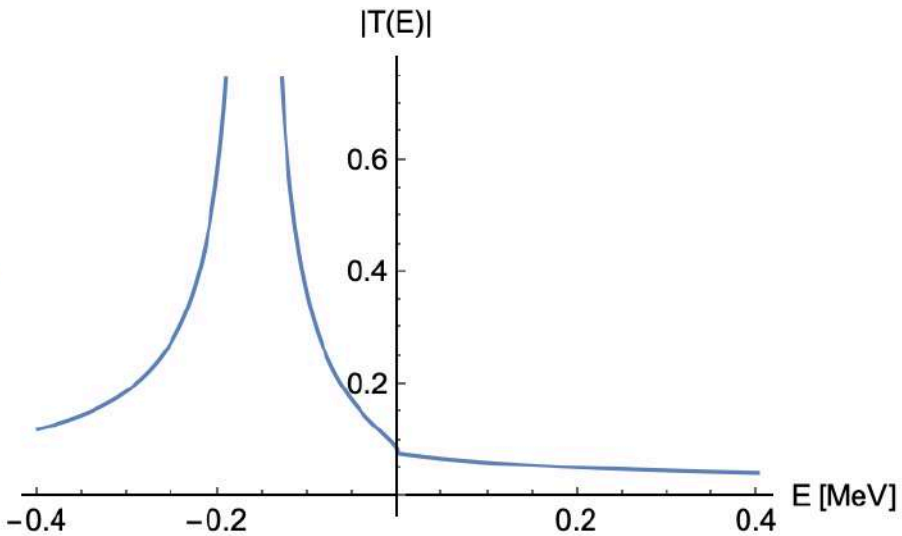

example pn, pp, nn : J=0

(this is not deuteron)

$V0=23$ MeV, $R=2$ fm, $m=m_N/2$

pole at $E \approx -160$ keV below th

in nature $E = -60$ keV

$E=p^2/2m$, $p=\pm\, i\sqrt{2m|E|}$, take -

the potential is just not deep enough

to form the bound state

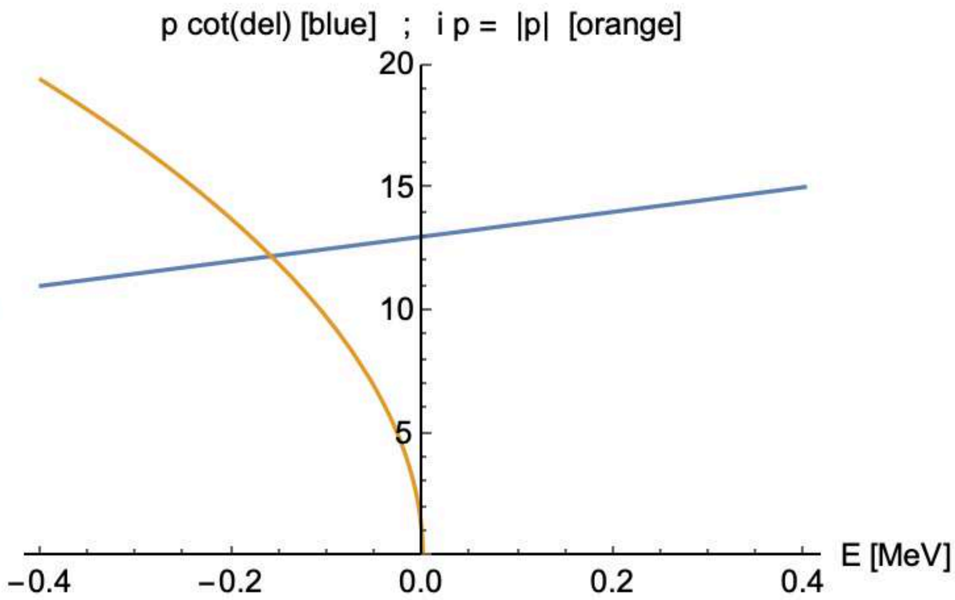

Large increase of rate above threshold

in case of shallow (virtual) bound state

$dN/dt \propto j\ \sigma \propto p\ |T|^2$

in both cases : pole below thresholds affects scattering above th.

example: deuteron (pn, J=1)

V0=36 MeV, R=2 fm, $m_r=m_N/2$

pole at E = $E_B = -2\ MeV$

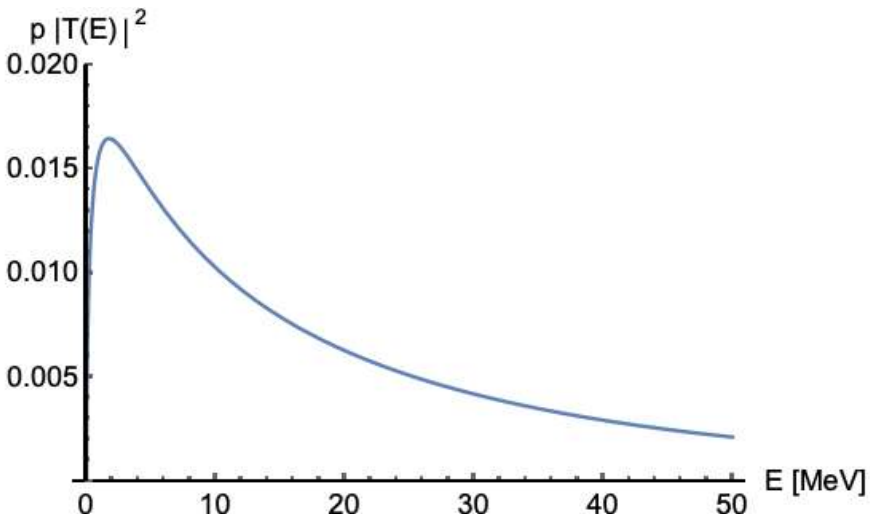

example pn, pp, nn : J=0

V0=23 MeV, R=2 fm, $m=m_N/2$

pole at E ≈ - 160 keV

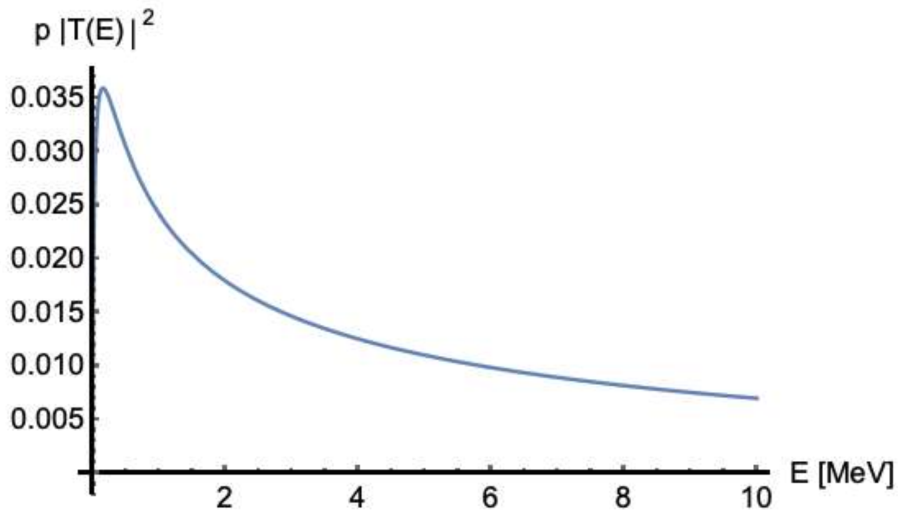

How to search for shallow bound state or virtual bound state on the lattice?

$$\boxed{T = \frac{1}{p \cot \delta_0 - ip}}$$

I'll show lattice exmaple of $D_{s0}^*(2317)$ bound state in DK scattering, s-wave

- extract T, δ or p cotδ as a function of E

  lat: these can be determined for real E above and somewhat below th.

  exp: real E above th. only

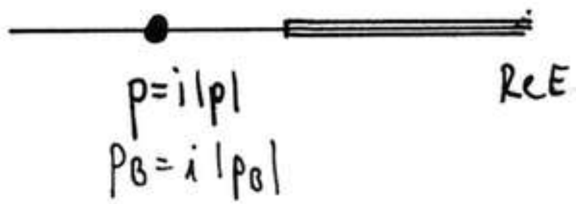

- bound state : pole in scattering matrix S or T for p=i |p|

  or p cotδ = i p = - |p|

- virtual bound state : pole in scattering matrix S or T for p= - i |p|

  or p cotδ = i p = |p|

before considering resonances

Intermezzo: 2 Rimann sheets & complex energies

relation between E and p outside the region of potential :

$E = p^2/2m$ E= $\sqrt{m_1^2 + p^2} + \sqrt{m_2^2 + p^2}$

p is obtained from E by taking square root: square root is multivalued function

p= $\mp\sqrt{2mE}$ $p = \pm\frac{1}{2}\sqrt{E^2 - 2(m_1^2 + m_2^2) + \frac{m_1^2 - m_2^2}{E^2}}$

so far we considered real E : E>0, E<0 : p= $\mp\sqrt{2mE}$, p= $\mp$ i |p|

in general one considers also complex E by continuing T(E) to the complex plane: again p is obtained from E

for given E : p has two values : Riemann sheet defines which of the two applies

Riemann sheet 1 (“physical”): Im(p)>0 Example: p=i|p| (bound state pole is on this sheet)

Riemann sheet 2 (“unphysical”): Im(p) <0 p=-i|p| (virtual bount st. pole is on this sh.)

Riemann sheet 1 (“physical”): Im(p)> 0

example: 2m=1 $p=\pm\sqrt{2mE} = \pm\sqrt{E}$

Riemann sheet 2 (“unphysical”): Im(p) <0

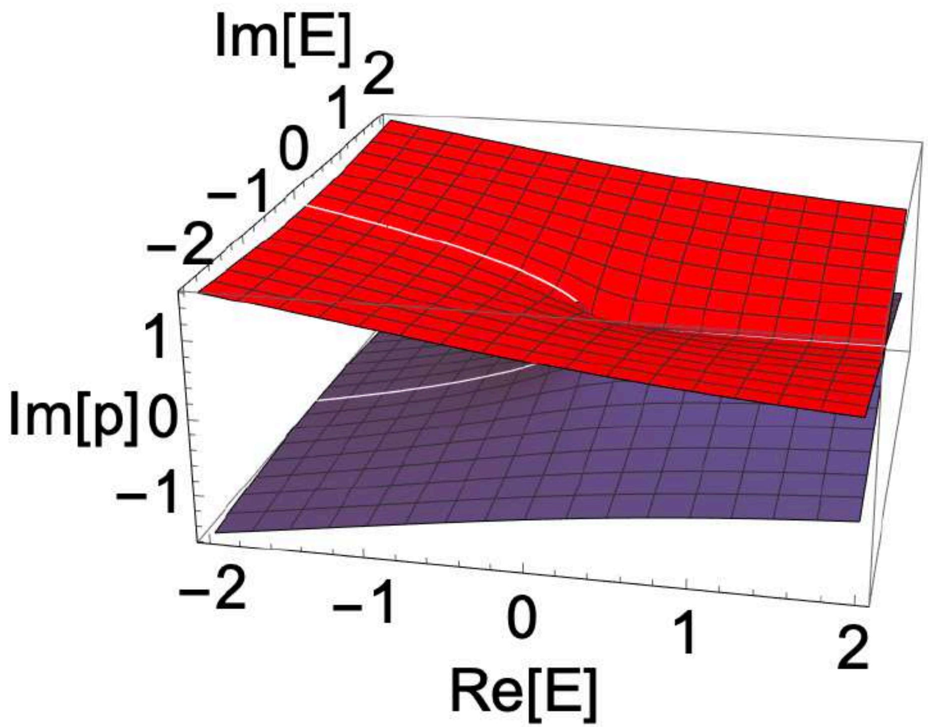

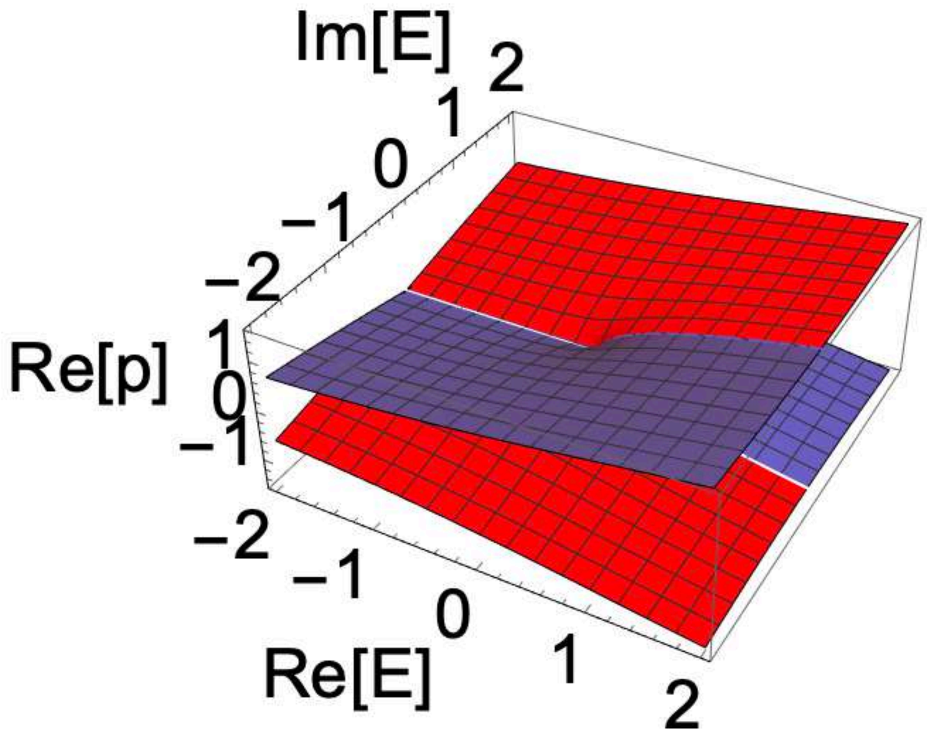


```
MySqrt[en_] := If[Im[Sqrt[en]] >= 0, Sqrt[en], -Sqrt[en]];

pval[en_, sheet_] := If[sheet == 1, MySqrt[en], -MySqrt[en]];
```

Riemann sheet 1 (“physical”): Im(p)> 0

location of apole in T for bound state pole

Riemann sheet 2 (“unphysical”): Im(p) <0

location of a pole in T for virtual bound state

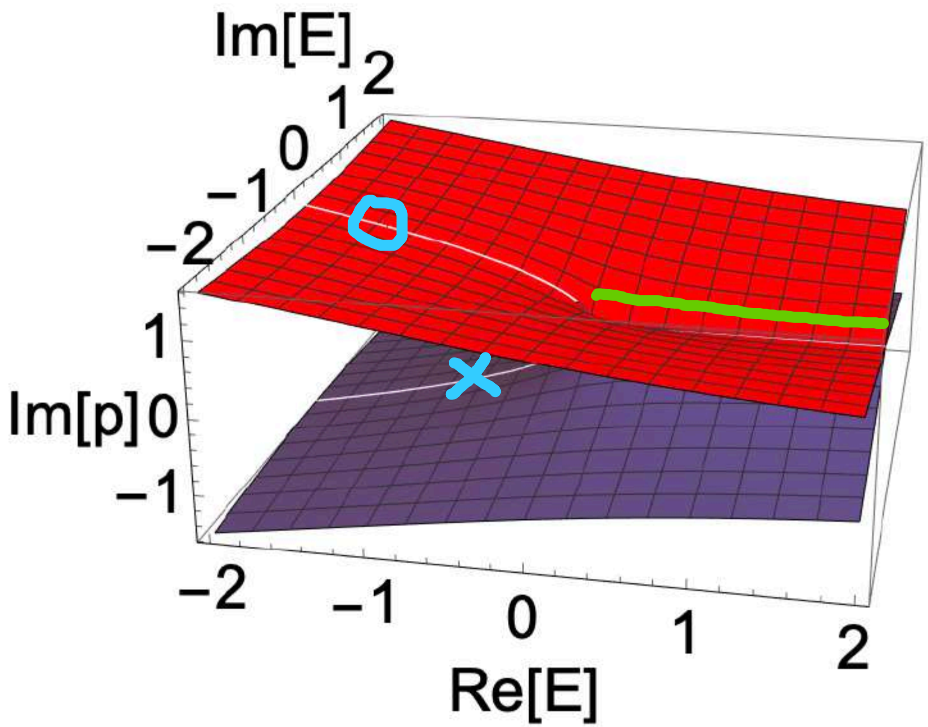

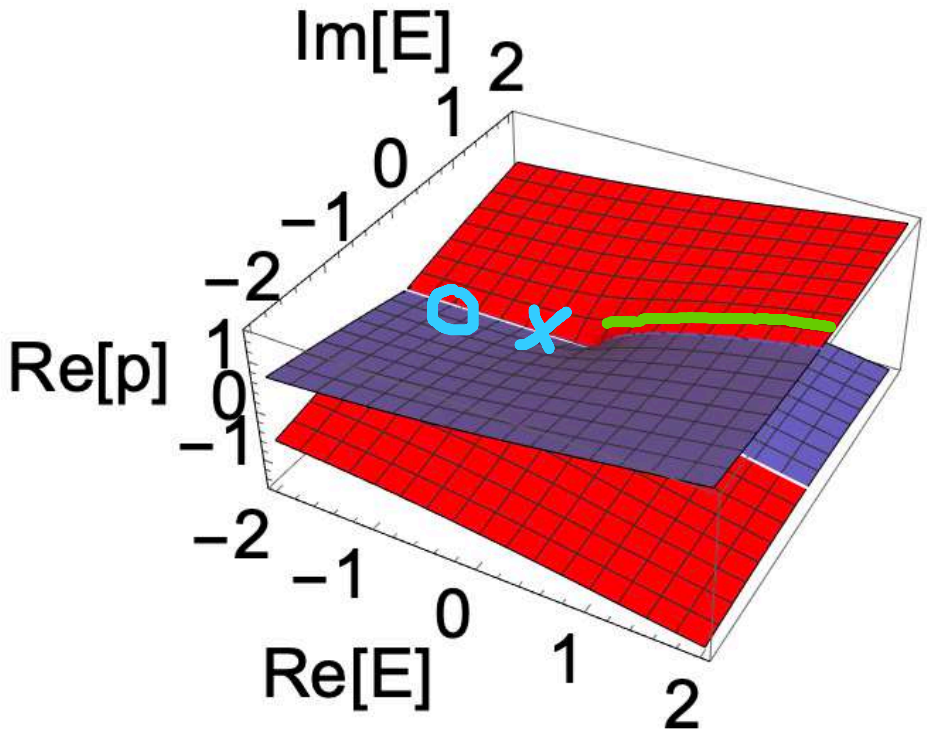

Experiments explore real E above threshold : E>0

Physical scattering : E=|E|+i eps

if poles are close below threshold:

they affect scattering in exp

Continued Intermezzo

Riemann sheet 1 (“physical”): Im(p)> 0

Riemann sheet 2 (“unphysical”): Im(p) <0

location of a pole in T

for a resonance (we will see that next)

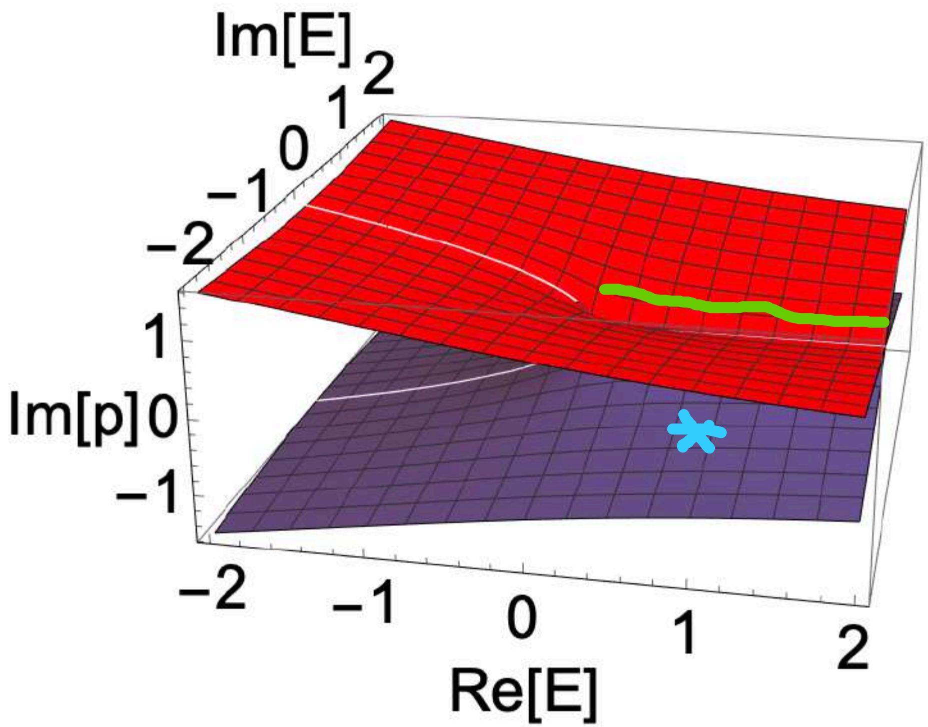

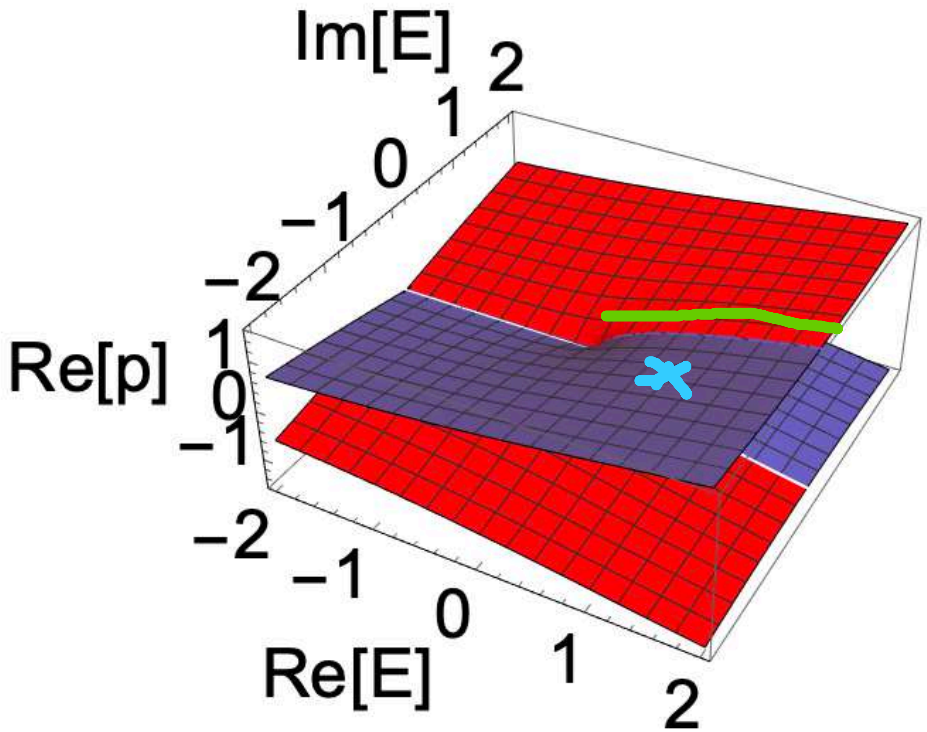

another view

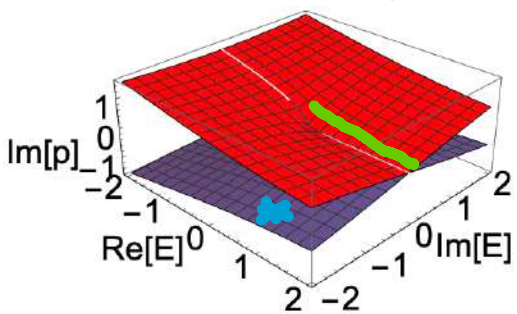

note: pysical axes is smoothly

connected to sheet II

If pole close to real axes:

affects scattering in exp.

$$\boxed{T = \frac{1}{p\cot\delta_0 - ip}}$$

poles of T are related to states:

(virtual) bound states and resonances

$$\boldsymbol{p\cot(\delta) = f(E)}$$

function of E, not of sqrt(E) : without proof

no sign ambiguity, same on both sheets

continuation to complex plane: E in f(E) replace by complex E

$\boldsymbol{i\,p}$:

sqrt(E), multivalued, the sign of this part depends on the sheet

continuation to complex plane: E in sqrt(E) replace by complex E:

Im(p)>0: sheet 1 ; Im(p)<0: sheet 2

focus on relativistic BW where $E=2\sqrt{m^2+p^2}$

Resonances: most hadrons are resonances

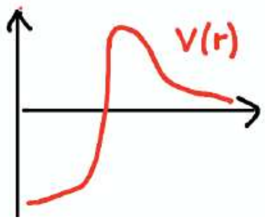

resonance s

Wednesday, 9 September 2020 21:05

$$\boxed{T=\frac{1}{p}\,\frac{1}{\cot\delta - i}} \qquad |T|^2 = \frac{1}{p^2}\,\frac{1}{\cot^2\delta + 1}$$

max: $\cot\delta = 0$, $\delta = \frac{\pi}{2}$, 90° phase shift at res. energy

parametrization: $\cot\delta = \dfrac{m_R^2 - E^2}{E\Gamma}$

- $E \simeq m_R$ $\delta = \pi/2$
- slope $\propto \Gamma$
- $E\uparrow$: $\cot\delta\downarrow$, $\delta\uparrow$

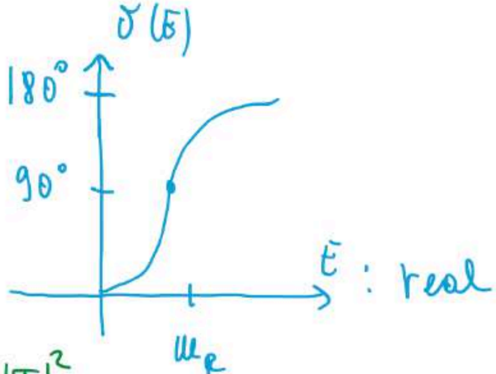

$$\boxed{T=\frac{1}{p}\,\frac{E\Gamma}{m_R^2 - E^2 - iE\Gamma}}$$

Breit Wigner resonance dependence

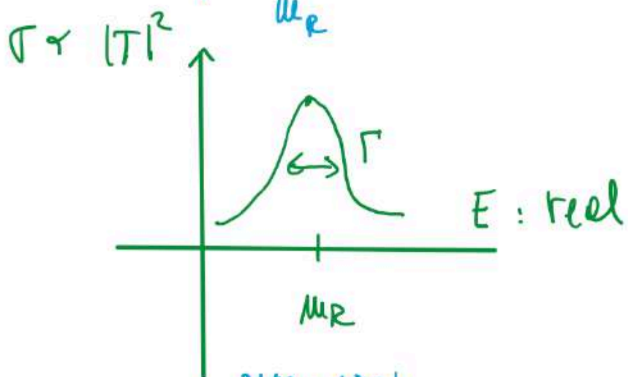

most comonly used quantity for res. in lat. sim.

$\Gamma \propto p^{2l+1}$ $\qquad \Gamma \equiv g^2\,\dfrac{p^{2l+1}}{E^2}$ $\qquad g$: coupling

$$\cot\delta = \frac{m_R^2 - E^2}{E\,g^2\,p^{2l+1}/E^2}$$

$$\boxed{\frac{p^{2l+1}\cot\delta}{E} = \frac{m_R^2 - E^2}{g^2}}$$

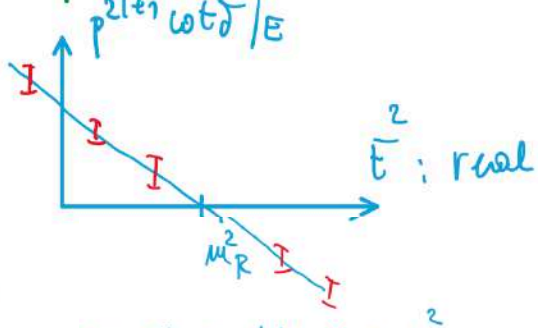

At real E: $T(E) \neq \infty$, no pole in T

crossing with 0 : m_R^2
slope $\to \Gamma$

focus on relativistic BW where E=$2\sqrt{m^2+p^2}$

Continuation of T(E) to complex E, pole

$$T=\frac{1}{p}\,\frac{E\Gamma}{m_R^2-E^2-iE\Gamma} \qquad E = \text{complex}$$

$$T=\infty \ : \ \text{pole} \ : \quad m_R^2-E^2-iE\Gamma=0 \qquad E^2+iE\Gamma-m_R^2=0$$

$$E=\frac{-i\Gamma\pm\sqrt{-\cancel{\Gamma^2}+4m_R^2}}{2}=\pm m_R-i\frac{1}{2}\Gamma \qquad E\simeq m_R-\frac{i}{2}\Gamma$$

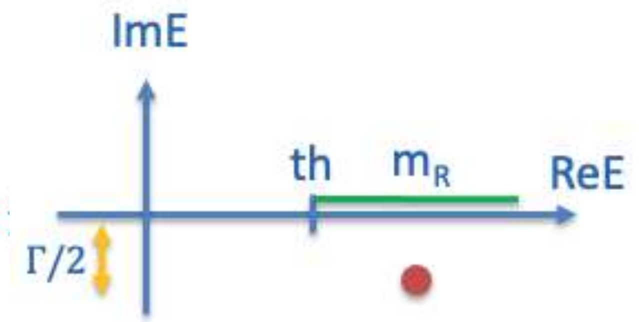

this pole affects $T(E_{ph})$

$E_{ph}=|E_{ph}|+i\epsilon$ physical axes

On which Riemann sheet is the pole located?

$\mathrm{Im}(p)\gtrless 0$ determine sign of $\mathrm{Im}(p)$ at the pole

$$T=\frac{1}{p\cot\delta-ip} \qquad ip=p\cot\delta=A-p^2B\,, \quad A,B>0$$

$\downarrow$

falling with E, p^2

$$Bp^2+ip-A=0$$

$$p=\frac{-i\pm\sqrt{-1+4AB}}{2B}\,, \quad \mathrm{Im}(p)<0$$

$$\boxed{\frac{p^{2\ell+1}\cot\delta}{E}=\frac{m_R^2-E^2}{g^2}}$$

this derivation applies for s-wave

and relativistic BW where E=$2\sqrt{m^2+p^2}$

p cot(del) = E ($m_R^2-E^2$)/g^2

~ const ($m_R^2-E^2$)

~ A – B p^2, A,B>0

[E depends very mildly on p in relativistic case]

Resonance corresponds to a pole in T on the second Riemann sheet.

T at this pole is smoothly connected to T on the physical axis: see plots on the slides. It significantly affects scattering in experiment (E_{ph}) if Γ not to large

The nonrelativistic derivation that resonance pole is at $E=m_R-i\,\Gamma/2$ on Riemann sheet II:

Perl, High Energy Hadron Physics, pages 345 (last paragraph) – 347.

At the end of lecture 1 I attach a pdf for pages 342-347,

which represent a self-contained derivation of poles in the complex energy plane

Note: T should have no poles away from real axis on sheet I: violation of causality

Summary: hadronic resonances appear in scattering as “bumps” in cross-section

decay time (via strong int.) : τ

uncertainty in E: $\Gamma = \hbar / \tau$

Γ=1–300 MeV

Example: ρ

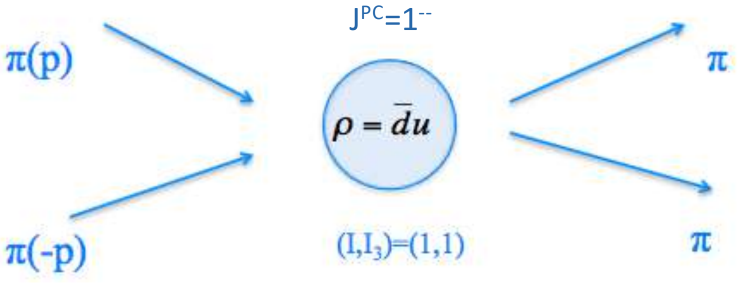

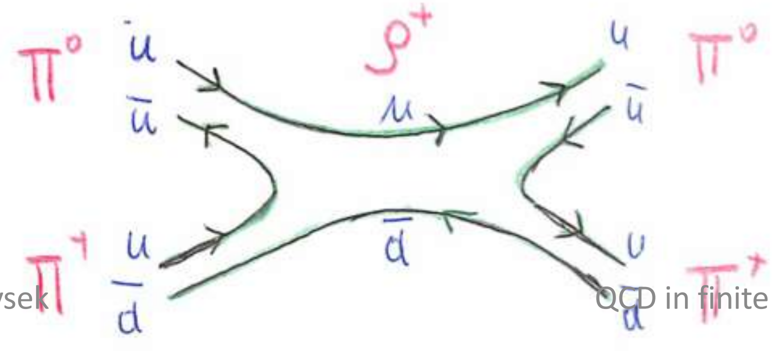

in experiment and in theory one determines:

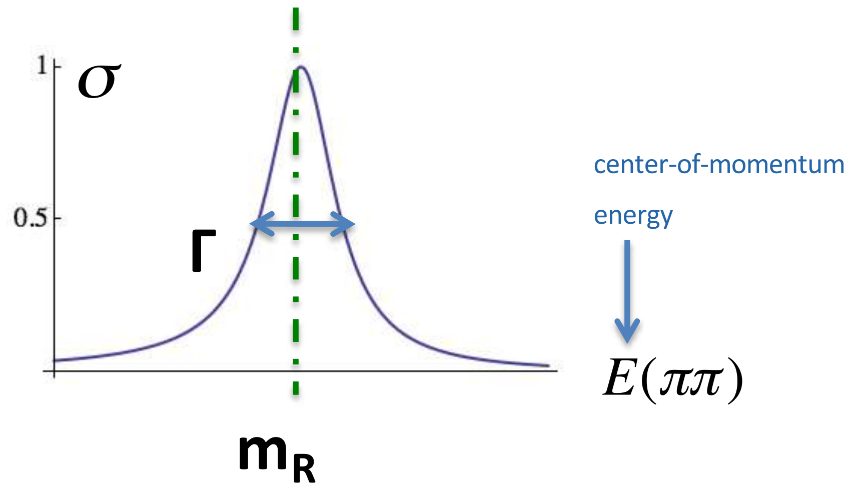

$$\sigma(E) \propto |T(E)|^2 = \left|\frac{E\Gamma}{E^2 - m_R^2 + iE\Gamma}\right|^2$$

simplest Breit Wigner

scattering matrix

What was covered last time ?

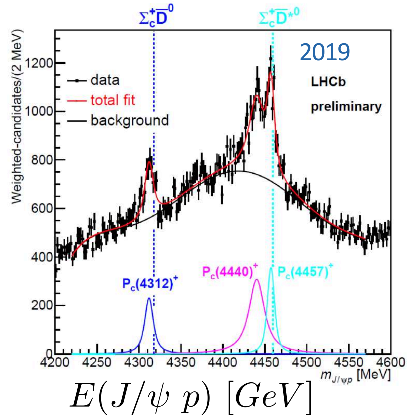

- most of hadrons are strongly decaying resonances

  they need to be inferred from scattering in exp or on the lattice

- two-hadron scattering in continuum

  so far s-wave (l=0)

  p momentum of particle in cmf

$$T = \frac{1}{p \cot \delta_0 - ip}$$

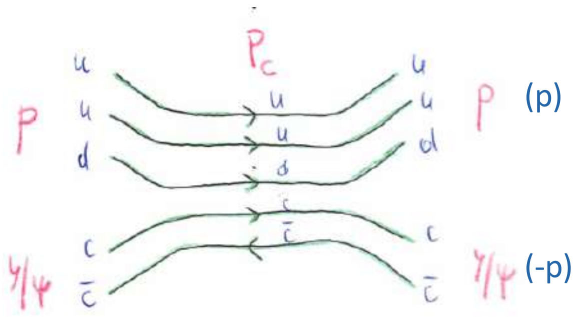

- real E -> complex E, E=E_{cm}

  Riemann sheet I if Im(p)>0

  Riemann sheet II if Im(p)<0

- location of pole in the scattering amplitude T(E) help to identify

  bound state: pole for real E below threshold Riemann sheet I

  virtual bound state: pole for real E below threshold Riemann sheet II

  resonance: pole away from real axes E=m-1/2 i Γ Riemann sheet II

  these poles affect physical scattering ("peaks in σ")

  if they are close to physical axes (green line) Riemann sheet I

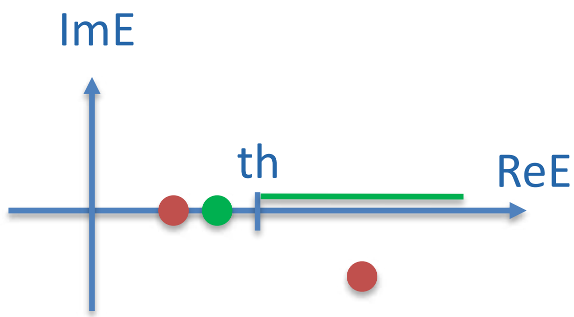

green: I red: II

Higher partial waves, l>0

$$\psi(r,\vartheta,\varphi) = R(r)\,Y_{lm}(\vartheta,\varphi)$$

$$\left[-\frac{\hbar^2}{2m}\frac{d^2}{dr^2}+\frac{\hbar^2 l(l+1)}{2mr^2}+V(r)\right]u(r)=Eu(r) \qquad R(r)=u(r)/r$$

inside:

R: complicated

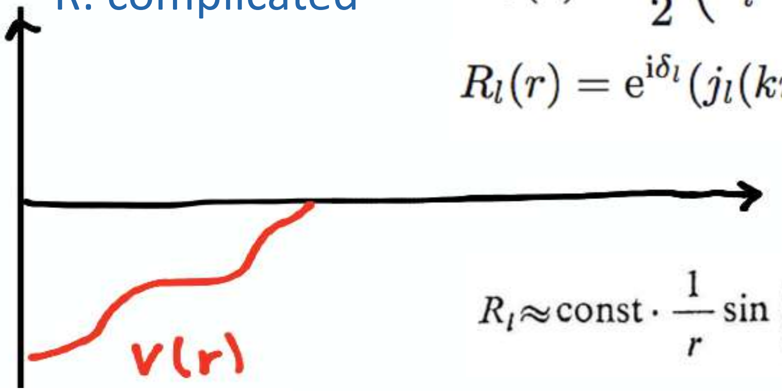

outside the region of potential

outgoing wave

$$R_l(r)=\frac{1}{2}\left(h_l^{(2)}(kr)+\mathrm{e}^{2\mathrm{i}\delta_l(E)}h_l^{(1)}(kr)\right)$$

$$R_l(r)=\mathrm{e}^{\mathrm{i}\delta_l}\left(j_l(kr)\,\cos\,\delta_l-n_l(kr)\,\sin\,\delta_l\right)$$

$$R_l \approx \text{const}\cdot\frac{1}{r}\sin\left(kr-\frac{\pi l}{2}+\delta_l\right)$$ for large r

$$S=e^{2i\delta_l}=1+2i\;p\;T$$

$SS^{+}=I$, S parametrized in terms of phase shift

$$\boxed{T=\frac{1}{p\cot\delta_l-ip}}$$

sometimes norm. of

T chosen diferently

solutions of ordinary diferential equations: tricvial with Mathematica NDSolve

$$\left[-\frac{\hbar^2}{2m}\frac{d^2}{dr^2}+\frac{\hbar^2 l(l+1)}{2mr^2}+V(r)\right]u(r)=Eu(r)$$

```
m = 1; l = 2; en = 0.5; V[r_] := -20 * Exp[-r^2]; eps = 10^(-5);
rep = NDSolve[
  {-u''[r] / (2 * m) + l * (l + 1) / (2 * m * r^2 + eps) * u[r] + V[r] * u[r] == en * u[r],
   u[0] == 0, u'[0] == 1}, u, {r, 0, 10}]
Plot[u[r] /. rep, {r, 0, 10}]
```

```
{{u → InterpolatingFunction[ Domain: {{0., 10.}} Output: scalar ]}}
```

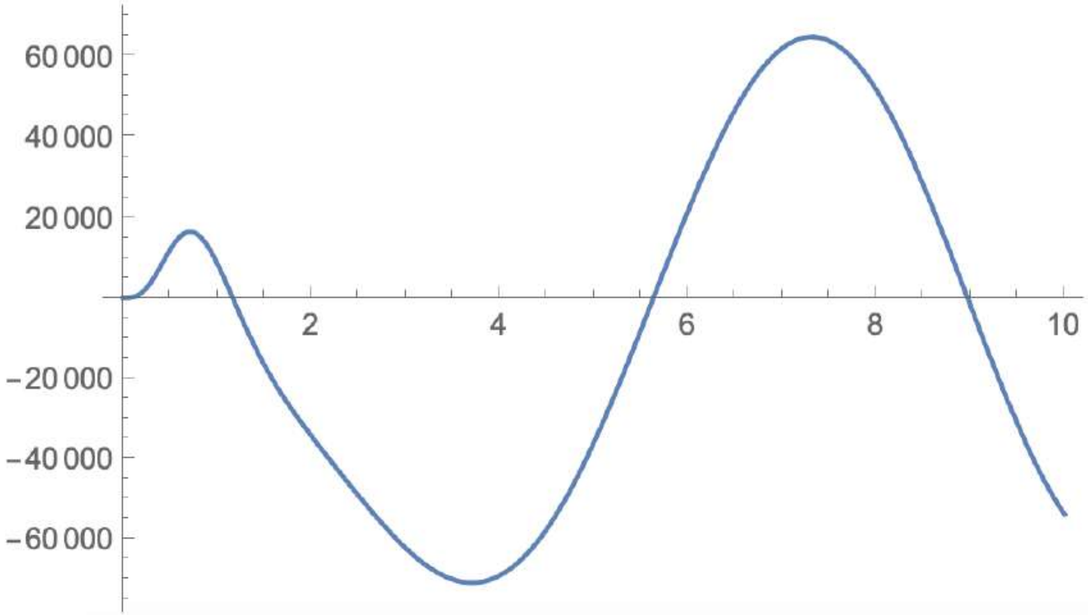

Screenshot

Near-threshold behavior of phase shift

Taylor expansion in p

for general potential and general partial wave l

$$\boxed{\lim_{p\to 0}\tan\delta_l(p) \propto p^{2l+1},} \quad \boxed{p^{2l+1}\cot\delta_l(p) = C + O(p^2)}$$

"Proof": Landau: QM, Sections 132 & 33, p -> k

$$\psi(r) = R_l(r) Y_{lm}$$

$$R_l = c_1(-1)^l \frac{(2l+1)!!}{k^{2l+1}} r^l \left(\frac{d}{r\,dr}\right)^l \frac{\sin kr}{r} + c_2(-1)^l \frac{r^l}{(2l-1)!!} \left(\frac{d}{r\,dr}\right)^l \frac{\cos kr}{r}.$$

kr >>1 : $$R_l \approx \frac{c_1(2l+1)!!}{rk^{l+1}} \sin\left(kr - \frac{\pi l}{2}\right) + \frac{c_2 k^l}{r(2l-1)!!} \cos\left(kr - \frac{\pi l}{2}\right)$$

kr >>1 : $$R_l \approx \mathrm{const} \cdot \frac{1}{r} \sin\left(kr - \frac{\pi l}{2} + \delta_l\right)$$

$$R_l \simeq \frac{const.}{r}\left[\ \cos\delta_l\ \sin(kr - \pi l/2) + \sin\delta_l\ \cos(kr - \pi l/2)\right]$$

$$\mathrm{tg}\,\delta_l \simeq \delta_l = \frac{c_2}{c_1 (2l-1)!!\,(2l+1)!!} k^{2l+1}$$

Effective range expansion

$$\boxed{p^{2l+1}\cot\delta_l(p) = C + O(p^2)} \qquad p^{2l+1}\cot\delta_l = C + D\,p^2 + E\,p^4 + ..$$

s-wave: $$p\cot\delta_0(p) = \frac{1}{a_0} + \frac{1}{2} r_0\, p^2$$ a0: scattering length

exercise: s-wave scattering on spherical potential well

$$\delta_0(p) = \arctan\left(\frac{p}{q}\tan(qR)\right) - pR + n\pi \qquad q = \sqrt{\underbrace{2\mu V_0}_{C^2} + p^2} = \sqrt{C^2 + p^2}$$

Taylor expanding

$$\boxed{p\cot\delta_0(p) =} \underbrace{\frac{C}{-C + \mathrm{Tan}[C]}}_{1/a_0} + \frac{1}{6}\left(3 - \frac{C^2}{(C - \mathrm{Tan}[C])^2} - \frac{3}{C^2 - C\,\mathrm{Tan}[C]}\right) p^2 + O[p]^4 \; \boxed{= \frac{1}{a_0} + \frac{1}{2} r_0\, p^2}$$

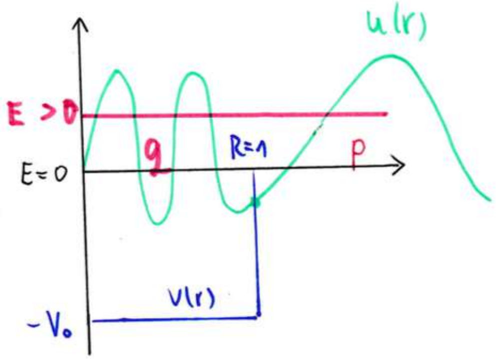

CHAPTER

15

Analyticity and Crossing in the Interaction of Spinless Particles

15-1 Introduction. For the last two decades elementary particle physicists have felt that the application of perturbation theory to strong interactions was an uncertain occupation, possibly a hopeless occupation. The qualitative successes of the one-particle exchange model must be balanced against the many quantitative failures. Therefore, particle physicists have tried to develop more fundamental approaches to strong interaction theory. And most of these approaches are based on or related to the treatment of scattering amplitudes as analytic functions.

As with so many other parts of strong interaction theory, we do not possess a rigorous and complete theory of the analytic properties of strong interaction amplitudes. Rather, we have constructed a loose theory based on different types of arguments and insights. To illustrate some of the origins of the theory, we

discuss the analytic properties of nonrelativistic partial wave amplitudes in Sec. 15-2 and perturbation theory and analyticity in Sec. 15-5; in Sec. 15-6 we show how the general unitarity relation relates to the singularities of the amplitude. We do not go into the derivation of analytic properties from axiomatic quantum field theory.

The incompleteness of the theory of the analytic behavior of amplitudes pervades not only the foundations of theory but also the applications of the theory. We cannot calculate an amplitude using the analytic properties alone because in general we do not know the residues and discontinuities at the singularities. We only know the position and nature of the singularities. Therefore the analytic nature of the amplitudes is used primarily as a guide and as a framework for describing the amplitudes. We illustrate this in Secs. 15-2 and 15-11 with the examples of bound states and resonances. Another illustration is provided by the development of the dispersion relation concept in Secs. 15-8 and 15-10.

15-2 Nonrelativistic Partial Wave Amplitudes and Analyticity. To begin our study we consider nonrelativistic elastic scattering, for by starting with nonrelativistic quantum mechanics we can most easily develop an understanding of the significance of the analytic properties of amplitudes. Consider a real, spherically symmetric potential $V(r) = (\hbar^2/2m)U(r)$. The radial Schrödinger equation for partial wave l, with $\psi(\mathbf{r}) = (u_l(k^2, r)/r)\, Y_l^m(\theta, \phi)$, is

$$\frac{d^2u_l(k^2, r)}{dr^2} + \left[k^2 - U(r) - \frac{l(l+1)}{r^2}\right]u_l(k^2, r) = 0 \tag{15-1}$$

where $k^2 = 2mE_{\text{kinetic}}$. We limit the form of $U(r)$ by requiring that as r approaches zero, $U(r)$ must not go to infinity as fast as $1/r^2$. As $r \to \infty$, however, $U(r)$ must go to zero faster than $1/r^2$. As $r \to 0$, $u_l(k^2, r)$ has two solutions

$$u_l(k^2, r) \xrightarrow[r\to 0]{} A_l r^{(l+1)} \tag{15-2a}$$

$$u_l(k^2, r) \xrightarrow[r\to 0]{} A_l r^{-l} \tag{15-2b}$$

Physically k^2 must be real and positive. But let us consider solutions of Eq. 15-1 for complex values of k^2. If these solutions $u_l(k^2, r)$ obey Eq. 15-2a, they are *regular analytic functions* of k^2 for finite values of r. That is, they are analytic functions without singularities in the complex k^2 plane. We apologize for not giving the proof of such an important statement, but the proof is based on the theory of differential equations and cannot be easily summarized here (15DE).

This sections shows that: if pole appears on sheet II away from real axes, this leads to BW form of T(E)

For scattering problems we are interested in the asymptotic form of $u_l(k^2, r)$. From Eq. 3-5 we have

$$u_l(k^2, r) \underset{r\to\infty}{\to} \frac{B_l}{2ik}\left[S_l(k^2)\, e^{ikr} - (-1)^l\, e^{-ikr}\right] \tag{15-3a}$$

or the alternate form

$$u_l(k^2, r) \underset{r\to\infty}{\to} \left[\phi_l^-(k^2)\, e^{ikr} + \phi_l^+(k^2)\, e^{-ikr}\right] \tag{15-3b}$$

We have only passing interest in $\Phi_l^{\pm}(k^2)$, the Jost functions, for we are really interested in using $\Phi_l^{\pm}(k^2)$ to study

$$S_l(k^2) = (-1)^{l+1}\,\frac{\Phi_l^-(k^2)}{\Phi_l^+(k^2)} \tag{15-4}$$

Our objective is to determine the analytic nature of $S_l(k^2)$ on the complex k^2 plane. As we shall see the singularities have direct physical significance.

But before we can do this we face an annoying task. Since Eq. 15-3 contains $k = \sqrt{k^2}$, which is a double-valued function of k^2, we must exercise care in associating a particular value of k with k^2. We write $k^2 = \kappa\, e^{i\phi}$ and $k = \kappa^{1/2}(\cos\phi/2 + i\sin\phi/2)$ where κ is real and positive and $0 \leqslant \phi \leqslant 4\pi$. Then we use two Riemann sheets to map k onto the k^2 plane; the sheets are defined below and pictured in Fig. 15-1. The k^2 plane is then cut along the real k^2 axis from zero to infinity.

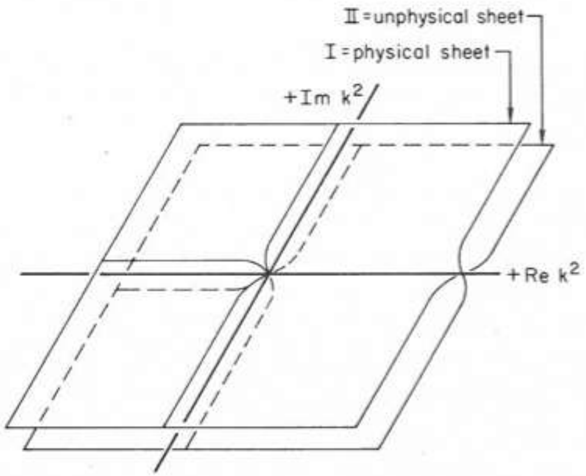

Fig. 15-1 The k^2 analytic plane for S_l, showing the two Riemann sheets.

sheet I, called the physical sheet, $\quad 0 \leqslant \phi \leqslant 2\pi, \quad \operatorname{Im} k > 0 \quad$ (15-5a)

sheet II, called the unphysical sheet, $\quad 2\pi \leqslant \phi \leqslant 4\pi, \quad \operatorname{Im} k < 0 \quad$ (15-5b)

The names physical sheet and unphysical sheet are more conventional than meaningful. In all our discussions of the analytic behavior of amplitudes, we have to describe how amplitudes for complex values of the kinematic parameters are connected with the physical amplitudes for the real values of the kinematic parameters. Here we adopt the convention

$$f(\operatorname{Re} k + i \operatorname{Im} k) \xrightarrow[\operatorname{Im} k \to 0]{} f_{\text{physical}}(\operatorname{Re} k) \qquad \text{for} \quad \operatorname{Im} k > 0 \tag{15-6}$$

Hence the designation of sheet I as the physical sheet. The information contained on both sheets is redundant, for taking $\Phi_l^{\pm}$ as functions of k we have

$$\Phi_l^+(k) = \Phi_l^-(-k) \tag{15-7a}$$

$$S_{lI}(k^2) = S_{lII}^{-1}(k^2) \tag{15-7b}$$

where the subscripts I, II denote the sheets.

Exercise 15-1. Derive Eq. 15-7 using Eq. 15-3b; then derive Eq. 15-8. See Ref. (15OMN).

In addition, the reality of the coefficients in Eq. 15-1 leads to the relations

$$\Phi_l^+(k^{2*}) = [\phi_l^+(k^2)]^*; \qquad \Phi_l^-(k^{2*}) = [\Phi_l^-(k^2)]^* \tag{15-8}$$

Examining the poles of $S_{lI}(k^2)$ in the complex k^2 plane, we see that $S_{lI}(k^2)$ will have a pole at k_0^2 if $\Phi_l^+(k^2)$ has a zero at that point. In that case, Eq. 15-3b reduces to

$$u_l(k_0^2, r) \underset{r\to\infty}{\to} \left[\Phi_l^-(k_0^2)\, e^{ir\operatorname{Re} k_0}\, e^{-br}\right] \tag{15-9}$$

Here $b = \operatorname{Im} k_0$, and b is positive according to Eq. 15-5a. Therefore, the right-hand side of Eq. 15-9 represents a wave function that is localized in space and normalizable. *If* k_0^2 is real and negative, the pole in $S_{lI}(k^2)$ at $k^2 = k_0^2$ represents a *bound state* of angular momentum *l*. We are in a nonrelativistic situation, and the binding energy of this bound state is simply $k_0^2/2m$. If a pole in $S_{lI}(k^2)$ occurs at a point not on the negative real k^2 axis, we cannot use this bound state interpretation; and there is no other physical significance to ascribe to such a pole. Indeed, conventional potentials do not produce poles in $S_{lI}(k^2)$ which are off the negative real k^2 axis. (See, however, Refs. 15OMN and 15FR.) Thus a pole in $S_{lI}(k^2)$ occurs only on the negative real k^2 axis and corresponds to a bound state.

Resonances ->

Next we consider the zeros of $\Phi^-(k^2)$. Suppose a zero occurs at $k_0^2 = \operatorname{Re} k_0^2 + i \operatorname{Im} k_0^2$, with $\operatorname{Re} k_0^2 > 0$ and $\operatorname{Im} k_0^2 > 0$. Then by Eqs. 15-4 and 15-7

$$S_{lI}(k^2) \text{ has zeros at } \operatorname{Re} k_0^2 \pm i \operatorname{Im} k_0^2 \tag{15-10a}$$

$$S_{lII}(k^2) \text{ has poles at } \operatorname{Re} k_0^2 \pm i \operatorname{Im} k_0^2 \tag{15-10b}$$

Let us further suppose that $\operatorname{Im} k_0^2 \ll \operatorname{Re} k_0^2$. Then the zero of S_{lI} at $\operatorname{Re} k_0^2 + i \operatorname{Im} k_0^2$ and the pole of S_{lII} at $\operatorname{Re} k_0^2 - i \operatorname{Im} k_0^2$ lie close to the point $k^2 = \operatorname{Re} k_0^2$ on the real k^2 axis.

Exercise 15-2. Fill in the steps in the arguments just presented. Use Eq. 15-5 to explain which zero and which pole lie close to the real k^2 axis.

The behavior of $S_l(k^2)$ in the vicinity of $k^2 = \operatorname{Re} k_0^2$ must be dominated by the nearby zero and pole. Hence for *real* values of k^2 near $\operatorname{Re} k_0^2$, the simplest form of S_l is

$$S_l(k^2) = \frac{k^2 - (\operatorname{Re} k_0^2 + i \operatorname{Im} k_0^2)}{k^2 - (\operatorname{Re} k_0^2 - i \operatorname{Im} k_0^2)} \tag{15-11a}$$

Note that Eq. 15-11a must and does fulfill the condition $|S_l^2| = 1$. We can bring Eq. 15-11a into a very familiar form by setting $E_0 = \operatorname{Re} k_0^2/2m$ and $\Gamma = \operatorname{Im} k_0^2/m$, giving

$$S_l(E) - 1 = \frac{-i\Gamma}{(E - E_0) + i\Gamma/2} \tag{15-11b}$$

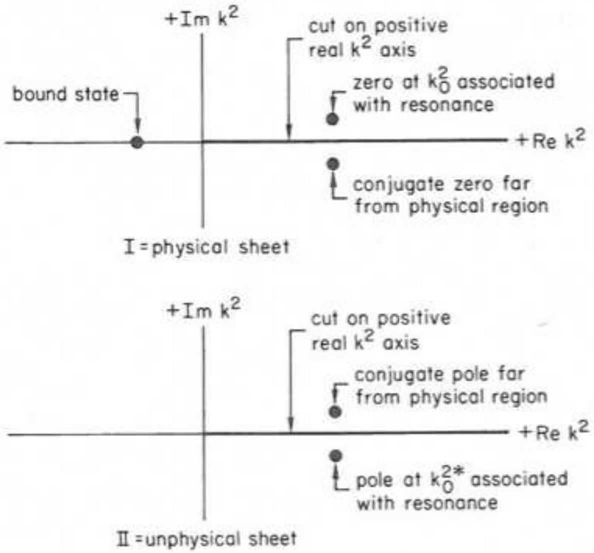

Fig. 15-2 Some singularities of S_l in the k^2 analytic plane.

which is the Breit-Wigner formula for a resonance! In Sec. 5-6 we gave a rather limited derivation of this formula. But the derivation offered here, which is based only on general ideas about the analytic properties of S, indicates the fundamental nature of the resonance concept. A resonance occurs whenever $S_{lII}(k^2)$ has a pole close to the real positive k^2 axis (also see Sec. 15-11).

As the pole in $S_{lII}(k^2)$ moves away from the real axis, the influence of the pole and the zero weakens, and other terms begin to dominate $S_l(E)$. From a more physical viewpoint, the Breit-Wigner curve becomes flatter and more difficult to detect. Thus a pole in $S_{lII}(k^2)$ that is far from the positive real axis cannot be given a direct physical significance.

In Fig. 15-2 we show the singularities discussed so far. Among singularities, not covered here is a very important branch point that occurs on the negative real k^2 axis. The position of this branch point and the discontinuity across the cut depend on the potential $U(r)$ in Eq. 15-1. But we must turn our attention to the relativistic problem, and we refer the reader to Refs. 15DE and 15OMN.

15-3 Two-Body Reactions–Kinematics and Cross Channels. To begin our study of the analyticity of relativistic amplitudes, we must discuss the kinematics that relate two-body crossed reactions. For a reaction $a + b \to c + d$, the *crossed*

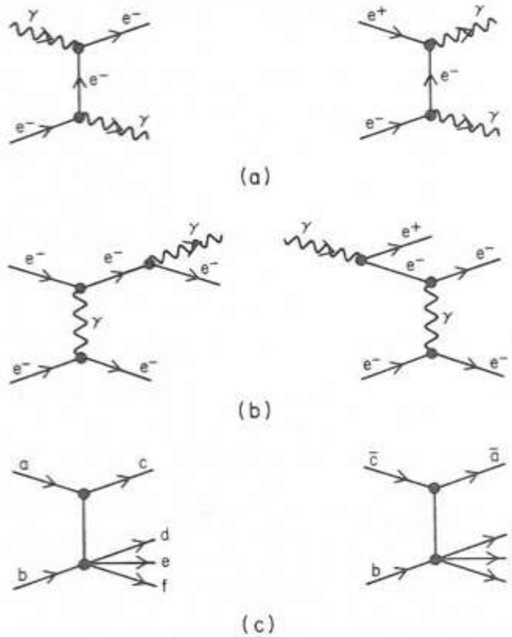

Fig. 15-3 Examples of crossed reactions in perturbation theory.